DALTON
FULL PAPER

Synthesis, characterization, crystal structures and reactivity of a series of ruthenium nitrene and nitrido carbonyl clusters containing bridging alkyne ligands

Emmie Ngai-Man Ho and Wing-Tak Wong *

Department of Chemistry, The University of Hong Kong, Pokfulam Road, Hong Kong, P.R. China

Received 3rd August 1998, Accepted 23rd October 1998

The reactions of $[Ru_3(CO)_9(\mu_3\text{-}CO)(\mu_3\text{-}NOMe)]$ **1** with alkynes, PhC_2R, in *n*-hexane afforded the new cluster $[Ru_3(CO)_9(\mu_3\text{-}NOMe)(\mu_3\text{-}\eta^2\text{-}RC_2Ph)]$ (**2a**, R = H; **2b**, R = Ph) in high yields. The molecules consist of an open triangular core of three metal atoms with triply bridging alkyne and μ_3-NOMe ligands on opposite sides of the cluster. Upon thermolysis in *n*-octane, $[Ru_4(CO)_9(\mu\text{-}CO)_2(\mu_4\text{-}NOMe)(\mu_4\text{-}\eta^2\text{-}HC_2Ph)]$ **3a**, $[Ru_4(CO)_9(\mu\text{-}CO)_2\{\mu_4\text{-}NC(O)OMe\}(\mu_4\text{-}\eta^2\text{-}HC_2Ph)]$ **4a** and $[Ru_5(CO)_{13}(\mu\text{-}CO)(\mu_4\text{-}NH)(\mu_4\text{-}\eta^2\text{-}HC_2Ph)]$ **5a** were isolated from **2a**, while $[Ru_4(CO)_9(\mu\text{-}CO)_2(\mu_4\text{-}NOMe)(\mu_4\text{-}\eta^2\text{-}PhC_2Ph)]$ **3b**, $[Ru_4(CO)_9(\mu\text{-}CO)_2\{\mu_4\text{-}NC(O)OMe\}(\mu_4\text{-}\eta^2\text{-}PhC_2Ph)]$ **4b**, $[Ru_4(CO)_9(\mu\text{-}CO)_2(\mu_4\text{-}NH)(\mu_4\text{-}\eta^2\text{-}PhC_2Ph)]$ **6b** and $[Ru_6(CO)_{13}(\mu\text{-}H)(\mu_5\text{-}N)(\mu_3\text{-}\eta^2\text{-}PhC_2Ph)_2]$ **7b** were obtained from **2b**. The structures of **3a**, **3b**, **4a** and **4b** consist of a slightly twisted square base of four metal atoms with quadruply bridging alkyne and μ_4-NOMe or μ_4-NC(O)OMe ligands on opposite sides of the clusters. Cluster **5a** has a structure analogous to that of **3a** with quadruply bridging phenylacetylene and μ_4-nitrene (NH) ligands but differs from **3a** due to the presence of a $Ru(CO)_4$ group on one edge of the tetraruthenium cluster, whilst cluster **7b** contains six ruthenium atoms and a μ_5-N nitrido atom. Five ruthenium atoms out of the six arrange in a novel wingtip-bridged metal skeleton. The binuclear metallapyrrolidone complex $[Ru_2(CO)_6\{\mu\text{-}\eta^3\text{-}HC_2(Ph)C(O)N(OMe)\}]$ **8a** was isolated from the direct reaction of **1** and phenylacetylene in refluxing *n*-octane, in which interaction of phenylacetylene with CO and the NOMe nitrene moiety was observed. Complex **3a** converts into **4a** in refluxing *n*-octane with or without bubbling CO. Substitution of MeCN with **3a** led to the activated $[Ru_4(CO)_8(\mu\text{-}CO)_2(NCMe)(\mu_4\text{-}NOMe)(\mu_4\text{-}\eta^2\text{-}HC_2Ph)]$ **9a** in moderate yields. Monosubstituted $[Ru_4(CO)_8(\mu\text{-}CO)_2(PPh_3)(\mu_4\text{-}NOMe)(\mu_4\text{-}\eta^2\text{-}HC_2Ph)]$ **10a** was isolated stoichiometrically when **9a** was stirred with PPh_3. However, direct substitution on **3a** with PPh_3 in the presence of Me_3NO gives disubstituted $[Ru_4(CO)_7(\mu\text{-}CO)_2(PPh_3)_2(\mu_4\text{-}NOMe)(\mu_4\text{-}\eta^2\text{-}HC_2Ph)]$ **11a** in addition to **10a**. Nucleophilic attack of H^- takes place on **3a** and **4a** and of I^- on **3a**, a terminal carbonyl ligand is replaced by these anionic ligands and the products were characterized by negative ionization fast atom bombardment mass spectrometry.

Introduction

The chemistry of transition metal clusters possessing μ_3-nitrene ligands has been extensively studied because of its role in the catalytic nitroarene carbonylation reactions.[1–3] The coupling of the nitrene ligand in $[Ru_3(CO)_9(\mu_3\text{-}CO)(\mu_3\text{-}NPh)]$ and alkynes is reported to give the metallapyrrolidone complex which further interacts thermally with an excess of alkyne and photochemically with carbon monoxide to give pentaphenylpyridone and 1,3,4-triphenylmaleimide respectively.[2] However, reports concerning μ_4-nitrene species are very rare. Blohm and Gladfelter[4] have shown that protonation of $[N(PPh_3)_2][Ru_4(CO)_{12}(\mu_4\text{-}N)]$ in the presence of diphenylacetylene gives a μ_4-NH containing species, $[Ru_4(CO)_9(\mu\text{-}CO)_2(\mu_4\text{-}NH)(\mu_4\text{-}\eta^2\text{-}PhC_2Ph)]$. Treatment of $[Ru_3(CO)_9(\mu\text{-}H)_2(\mu_3\text{-}NPh)]$ with diphenylacetylene was found to produce the μ_4-nitrene cluster $[Ru_4(CO)_9(\mu\text{-}CO)_2(\mu_4\text{-}NPh)(\mu_4\text{-}\eta^2\text{-}PhC_2Ph)]$.[5] Alkynes are important structural stabilizers in the formation and isolation of the μ_4-nitrene containing clusters. In our efforts to develop the chemistry of μ_4-nitrene ligands in metal clusters, we have previously demonstrated the syntheses of a series of ruthenium μ_4-nitrene carbonyl clusters prepared from the thermolysis or pyrolysis of $[Ru_3(CO)_9(\mu_3\text{-}CO)(\mu_3\text{-}NOMe)]$ **1**.[6] Herein, we report the reactivity of alkynes towards **1**, which resulted in the isolation of a series of nitrene clusters in more accessible yields. A preliminary report on part of this work has been published.[7]

Results and discussion

Reactions of $[Ru_3(CO)_9(\mu_3\text{-}CO)(\mu_3\text{-}NOMe)]$ 1 with alkynes in *n*-hexane

The reactions of $[Ru_3(CO)_9(\mu_3\text{-}CO)(\mu_3\text{-}NOMe)]$ **1** with phenylacetylene (PhC_2H) and diphenylacetylene (PhC_2Ph) in *n*-hexane at 60 °C led to the formation of $[Ru_3(CO)_9(\mu_3\text{-}NOMe)(\mu_3\text{-}\eta^2\text{-}RC_2Ph)]$ (**2a**, R = H; **2b**, R = Ph) in high yields (Scheme 1). This offered the opportunity to study the reactivities of clusters **2a** and **2b**. They were fully characterized by conventional spectroscopic techniques [IR, ^1H, ^{15}N NMR and fast atom bombardment (FAB) mass spectrometry] and elemental analyses, see Table 1. The IR spectra reveal that only terminal carbonyl ligands are present. The positive FAB mass spectra displayed molecular ion peaks at *m/z* 702 and 778 and daughter ions due to successive loss of nine carbonyls. In the ^1H NMR spectra, apart from the multiplets [δ 7.12–6.80] due to the phenyl groups, there are sharp singlets at δ 8.34 and 3.36 for **2a** and δ 3.44 for **2b**. The low field signal was assigned to the acetylenic proton in **2a**. The ^{15}N NMR spectra exhibited a resonance at δ 345.9 and 341.5 (relative to liquid NH_3) for **2a** and **2b** respectively.

In order to establish the molecular structures of clusters **2a** and **2b**, single-crystal X-ray diffraction analyses were carried out. Bright yellow crystals were obtained by slow evaporation of a saturated solution of *n*-hexane and a

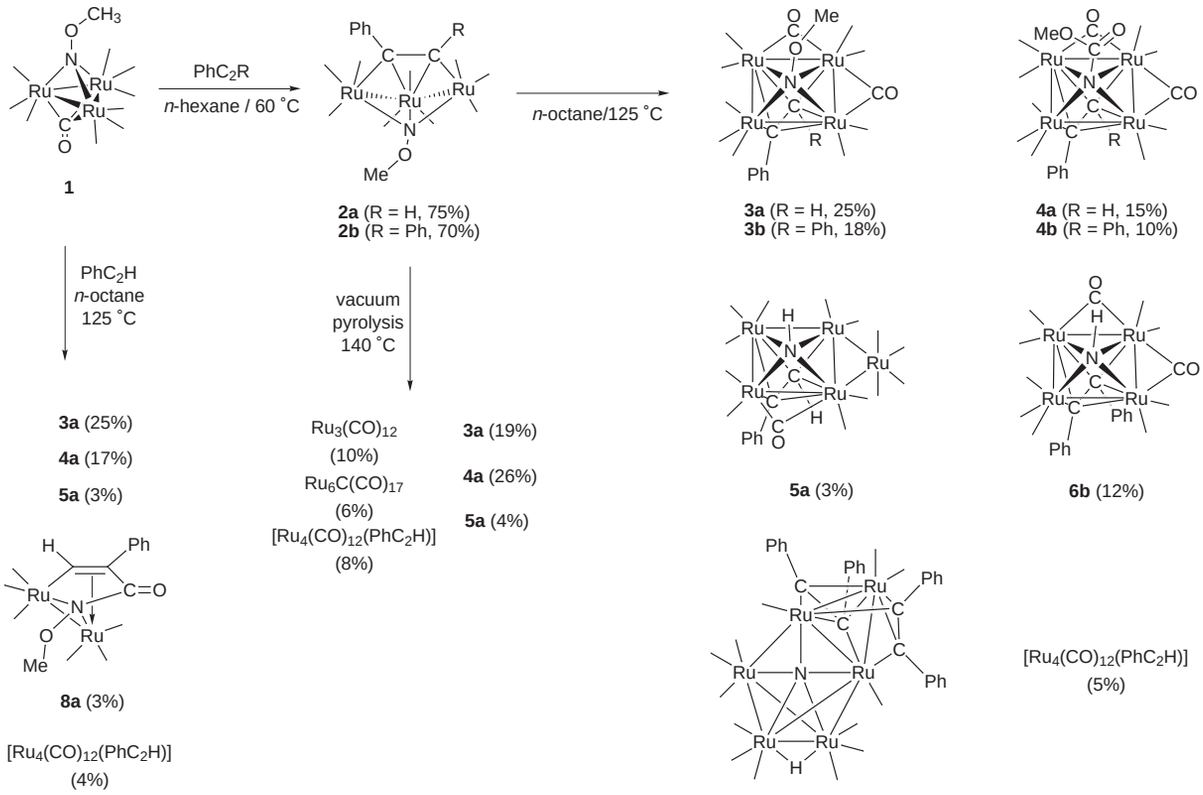

Scheme 1

Table 1 Spectroscopic data for compounds **1**–**14**

Cluster	IR Spectra [a] ν(CO)/cm^{-1}	Mass spectra [b] (m/z)	^{1}H NMR spectra [c] (δ, J/Hz)	^{15}N NMR spectra [d] (δ, J/Hz)
1	2103w, 2069vs, 2034vs, 2015s, 1741m	602(628) [e]	3.45 (s, 3 H)	287.3 (s)
2a	2097w, 2076vs, 2055vs, 2028vs, 2007s, 1999 (sh)	702(702)	8.34 (s, 1 H), 7.12 (m, 3 H), 7.00 (m, 2 H), 3.36 (s, 3 H)	345.9 (s)
2b	2095w, 2076vs, 2047vs, 2030vs, 2006s, 1993 (sh)	778(778)	6.96 (m, 4 H), 6.80 (m, 6 H), 3.44 (s, 3 H)	341.5 (s)
3a	2091w, 2060s, 2037vs, 2010m, 1993w, 1981w, 1912w, 1852m	859(859)	7.02 (m, 3 H), 6.36 (m, 2 H), 3.82 (s, 1 H), 1.74 (s, 3 H)	308.0 (s)
3b	2089w, 2062s, 2037s, 3032vs, 2016m, 1989m, 1979w, 1906w, 1850m	935(935)	6.74 (m, 6 H), 5.97 (m, 4 H), 1.78 (s, 3 H)	301.6 (s)
4a	2093w, 2060s, 2049vs, 2039m, 2028m, 2010m, 1997w, 1912w, 1858m [1686w (KBr disc)]	859(887) [e]	7.02 (m, 3 H), 6.32 (m, 2 H), 4.13 (s, 1 H), 2.93 (s, 3 H)	52.8 (s)
4b	2093w, 2062vs, 2047vs, 2039m, 2028m, 2014m, 1995m, 1906w, 1858m [1700w (KBr disc)]	963(963)	6.74 (m, 6 H), 5.89 (m, 4 H), 2.96 (s, 3 H)	79.9 (s)
5a	2105w, 2072s, 2043s, 2037vs, 2030s, 2014w, 2005w, 1985w, 1954w, 1893vw	1014(1014)	7.15 (m, 3 H), 6.77 (m, 2 H), 4.78 (s, 1 H), 3.72 (t, J_{NH} = 47.19, 1 H)	—
6b	2087w, 2060s, 2051w, 2033vs, 2024m, 2010m, 1983m, 1898w, 1856m	905(905)	6.64 (m, 6 H), 5.82 (m, 4 H), 1.87 (t, J_{NH} = 50.71, 1 H)	47.6 [d, J(^{15}NH) = 70.54]
7b	2097w, 2082m, 2062m, 2037s, 2028vs, 2005m, 1966w	1341(1341)	7.07 (m, 10 H), −22.68 (s, 1 H)	549.8 (s)
8a	[2097s, 2068vs, 2026vs, 2003s (CH_2Cl_2)] [1711m (KBr disc)]	545(545)	8.72 (s, 1 H), 7.72 (m, 2 H), 7.37 (m, 3 H), 3.46 (s, 3 H)	—
9a	2060w, 2035s, 2026vs, 2001m, 1978m, 1960vw, 1900vw, 1841w, 1736w	872(872)	**9a**: 6.90 (m, 3 H), 6.13 (m, 2 H), 5.03 (s, 1 H), 2.16 (s, 3 H), 1.73 (s, 3 H) **9a′**: 6.98 (m, 3 H), 6.47 (m, 2 H), 2.69 (s, 1 H), 2.11 (s, 3 H), 1.73 (s, 3 H)	—
10a [f]	2066w, 2035m, 2026vs, 2008w, 1974w, 1952vw, 1895vw, 1842w	1093(1093)	7.82 (m, 6 H), 7.53 (m, 9 H), 6.78 (m, 3 H), 5.94 (s, 1 H), 5.84 (m, 2 H), 1.81 (s, 3 H)	280.6 (s)
11a [g]	2008vs, 1954m, 1858w, 1808w	1327(1327)	7.80 (m, 6 H), 7.50 (m, 9 H), 7.34 (m, 15 H), 6.67 (m, 3 H), 5.90 (s, 1 H), 5.77 (m, 2 H), 1.15 (s, 3 H)	291.3 (s)
12	2091w, 2076w, 2060s, 2037vs, 2008s, 1993m, 1981m, 1911w, 1852m	845(873) [e]	6.82 (d, J_{HH} = 8.07, 2 H), 6.27 (d, J_{HH} = 8.07, 2 H), 3.68 (s, 1 H), 2.17 (s, 3 H), 1.73 (s, 3 H)	308.25 (s)
13	2089w, 2059vs, 2049s, 2037vs, 2026m, 2008m, 1987m, 1904w, 1856m [3347w (KBr disc)]	843(843)	6.79 (m, 2 H), 6.20 (m, 2 H), 3.86 (s, 1 H), 2.17 (s, 3 H), 1.96 (t, J_{NH} = 49.3, 1 H)	53.13 [d, J(^{15}NH) = 70.64]
14	Identical to **13**	901(901)	6.79 (m, 2 H), 6.20 (m, 2 H), 3.94 (s, 1 H), 2.94 (s, 3 H), 2.17 (s, 3 H)	87.12 (s)

[a] In *n*-hexane unless otherwise stated. [b] Calculated values in parentheses. [c] In CD_2Cl_2. [d] In $CDCl_3$, with ^{1}H decoupled except for clusters **6b** and **13**. [e] Only $[M - CO]^+$ is observed. [f] ^{31}P NMR ($CDCl_3$, ^{1}H decoupled) δ 46.89 (s). [g] ^{31}P NMR ($CDCl_3$, ^{1}H decoupled) δ 48.47 (d, J_{pp} 6.96) and 28.92 (d, J_{pp} 6.96 Hz).

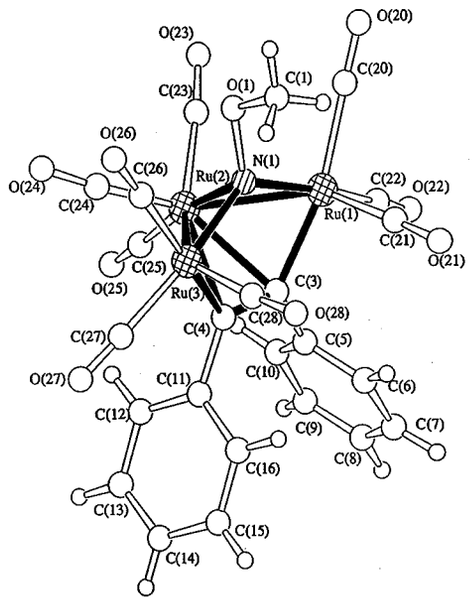

Fig. 1 The molecular structure of $[Ru_3(CO)_9(\mu_3\text{-}NOMe)(\mu_3\text{-}\eta^2\text{-}RC_2Ph)]$ illustrated by **2b** (R = Ph); the structure of **2a** (R = H), and its atom numbering scheme, are very similar but with the phenyl ring attached to C(4) replaced by an H atom.

Table 2 Selected bond lengths (Å) and angles (°) for compounds **2a** and **2b**

	2a	**2b**
Ru(1)–Ru(2)	2.725(1)	2.7456(2)
Ru(2)–Ru(3)	2.738(1)	2.7256(5)
Ru(1)–N(1)	2.056(7)	2.052(3)
Ru(2)–N(1)	2.088(7)	2.096(3)
Ru(3)–N(1)	2.058(7)	2.035(3)
Ru(1)–C(3)	2.069(8)	2.080(4)
Ru(2)–C(3)	2.304(8)	2.358(4)
Ru(2)–C(4)	2.295(8)	2.310(4)
Ru(3)–C(4)	2.040(9)	2.073(4)
N(1)–O(1)	1.416(9)	1.453(4)
O(1)–C(1)	1.43(1)	1.425(4)
C(3)–C(4)	1.42(1)	1.414(5)
Ru(1)–Ru(2)–Ru(3)	85.21(3)	85.15(2)
Ru(1)–N(1)–Ru(2)	82.2(3)	82.9(2)
Ru(1)–N(1)–Ru(3)	128.0(4)	129.8(2)
Ru(2)–N(1)–Ru(3)	82.7(3)	82.6(1)
Ru(1)–C(3)–C(4)	121.3(6)	122.8(3)
Ru(3)–C(4)–C(3)	126.1(6)	124.1(3)

n-hexane–dichloromethane solution at −20 °C respectively. The molecular structure is depicted in Fig. 1, while selected bond distances and angles are given in Table 2. Ruthenium clusters possessing a methoxynitrido moiety are rare and limited to **1** and the hydrido-derivative $[Ru_3(\mu\text{-}H)_2(CO)_9(\mu_3\text{-}NOMe)]$. The molecular structures of **2a** and **2b** are unprecedented and they are the first structural examples of a trinuclear methoxynitrido cluster with an open trimetallic core. Both **2a** and **2b** consist of an open triangular metal core [Ru(1)–Ru(2) 2.725(1) and Ru(2)–Ru(3) 2.738(1) Å for **2a**; Ru(1)–Ru(2) 2.7456(5) and Ru(2)–Ru(3) 2.7256(5) Å for **2b**] which is capped on both sides by a triply bridging methoxynitrido ligand and a triply bridging alkyne ligand similar to the geometry of $[Ru_3(CO)_9(\mu_3\text{-}S)(\mu_3\text{-}\eta^2\text{-}HC_2Ph)]$[8] or $[Fe_3(CO)_9(\mu_3\text{-}PC_6H_4OMe)(\mu_3\text{-}\eta^2\text{-}HC_2Ph)]$.[9] The μ_3-methoxynitrido moiety is capped symmetrically above the open triruthenium core with an open Ru···Ru separation of 3.698(1) and 3.7016(5) Å for **2a** and **2b** respectively, while the alkyne ligand is capped on the other face of the triruthenium core with the carbon C(3) bonded to Ru(1) and Ru(2) and carbon C(4) bonded to Ru(2) and Ru(3). The C(3)–C(4) bond distances in the alkyne ligands at 1.42(1) Å for **2a** and 1.414(5) Å for **2b** are typical of those observed for triply bridging alkyne ligands. The phenyl rings attached on the co-ordinated alkyne ligands exhibit proton resonances at the expected region for the phenyl groups while the hydrogen atom on C(4) in **2a** shows a characteristic resonance, δ 8.34, in the ^{1}H NMR spectrum which is consistent with previously reported values.[8,9] The structures of **2a** and **2b** can also be viewed as a pentagonal pyramid with an equatorial plane containing two Ru atoms, the acetylene carbons and the nitrene N atom. This plane is capped by one $Ru(CO)_3$ unit. The five atoms Ru(1), N(1), Ru(3), C(4) and C(3) in the equatorial plane are essentially coplanar with the mean deviations of 0.1149 and 0.1023 Å for **2a** and **2b** respectively from the least-squares plane. The vertices Ru(2) atoms lie 1.94 and 1.95 Å above their basal planes. Both methoxynitrido and alkyne moieties act as four-electron donors which results in a total of 50 cluster valence electrons and is consistent with the observation of only two formal Ru–Ru bonds in the trinuclear framework.

Thermolysis of $[Ru_3(CO)_9(\mu_3\text{-}NOMe)(\mu_3\text{-}\eta^2\text{-}HC_2Ph)]$ 2a

Heating compound **2a** in refluxing *n*-octane for 3 h afforded a dark brown mixture. Three new μ_4-nitrene carbonyl clusters, $[Ru_4(CO)_9(\mu\text{-}CO)_2(\mu_4\text{-}NOMe)(\mu_4\text{-}\eta^2\text{-}HC_2Ph)]$ **3a**, $[Ru_4(CO)_9(\mu\text{-}CO)_2\{\mu_4\text{-}NC(O)OMe\}(\mu_4\text{-}\eta^2\text{-}HC_2Ph)]$ **4a** and $[Ru_5(CO)_{13}(\mu\text{-}CO)(\mu_4\text{-}NH)(\mu_4\text{-}\eta^2\text{-}HC_2Ph)]$ **5a** were isolated in 25%, 15% and 3% yields along with a small amount of the known cluster $[Ru_4(CO)_{12}(\mu_4\text{-}\eta^2\text{-}HC_2Ph)]$[10] (Scheme 1). Clusters **3a**, **4a** and **5a** were characterized by various spectroscopic methods (Table 1). The IR spectra show the presence of both terminal and bridging carbonyl ligands and all the mass spectra exhibit molecular ion envelopes which agree with the formulae of the compounds, with ion peaks corresponding to CO losses also being present. Moreover the ^{1}H NMR signals due to the organic moieties of all these three complexes are fully consistent with their structures. The signals due to protons of the phenyl rings are observed in the range δ 7.15–6.32 and the resonances for the acetylenic protons in **3a**, **4a** and **5a** occur at δ 3.82, 4.13 and 4.78 respectively. The μ_4-methoxynitrido group in **3a** gives a signal at δ 1.74 for the methoxy protons, which is relatively upfield of the μ_3-methoxynitrido protons. The signal at δ 2.93 in the ^{1}H NMR spectrum of **4a** is assigned to methoxy group protons in the carbamate derivative. The ^{1}H NMR spectrum of **5a** shows a triplet centred at δ 3.72 with a coupling constant of 47.2 Hz which may be attributable to the NH proton. The ^{15}N NMR studies of the ^{15}N-enriched samples of **3a** and **4a** give singlets at δ 308.0 and 52.8 accordingly. The ^{15}N NMR study of **5a** was hindered due to the low yield. The structures of complexes **3a**, **4a** and **5a** have been established by X-ray crystallographic studies.

Yellow crystals of clusters **3a** and **4a** and blue crystals of **5a** suitable for diffraction studies were grown from a saturated solution of *n*-hexane–*n*-octane at −20 °C. The molecular structures of **3a** and **4a** are depicted in Figs. 2 and 3 and relevant structural parameters are listed in Table 3. The molecular geometries of clusters **3a** and **4a** are similar in that the four ruthenium atoms are arranged as a slightly twisted square base with a quadruply bridging PhC_2H ligand. The metal core can be described as a rhombus with four Ru–Ru bonds. Both of them have two CO-bridged Ru–Ru bonds [average 2.6838(7) for **3a** and 2.692(1) Å for **4a**] and two non-bridged Ru–Ru bonds [average 2.7654(7) for **3a** and 2.766(5) Å for **4a**]. There are no isomeric molecules with differences in the alkyne orientation for **3a** and **4a** or for the following structures. In the reactions involving tolylacetylene[7] the analogous product of **4a**, having the μ_4-NC(O)OMe moiety, is present as two isomers.

The mean deviations of the plane defined by the four metal atoms are 0.2031 [**3a**] and 0.1800 Å [**4a**], respectively. These molecules are structurally similar to the compounds $[Ru_4(CO)_9(\mu\text{-}CO)_2(\mu_4\text{-}PPh)(\mu_4\text{-}\eta^2\text{-}PhC_2Ph)]$[11] and $[Ru_4(CO)_9$-

Table 3 Selected bond lengths (Å) and angles (°) for compounds **3a**–**5b** and **9a**–**11a**; the values in square brackets refer to the second independent molecule of **10a**

	3a	**3b**	**4a**	**4b**	**5a**	**9a**	**10a**		**11a**
Ru(1)–Ru(2)	2.8021(7)	2.7278(4)	2.807(1)	2.7398(9)	2.6983(5)	2.786(1)	2.6967(6)	[2.6876(7)]	2.678(2)
Ru(1)–Ru(4)	2.7287(7)	2.7920(4)	2.724(1)	2.7445(8)	2.7615(5)	2.723(1)	2.6703(6)	[2.6742(6)]	2.686(2)
Ru(2)–Ru(3)	2.6945(7)	2.6830(4)	2.699(1)	2.6988(8)	2.6589(5)	2.700(2)	2.8161(6)	[2.7985(6)]	2.805(2)
Ru(3)–Ru(4)	2.6731(7)	2.6910(4)	2.685(1)	2.7076(9)	2.7772(5)	2.676(1)	2.7933(6)	[2.8188(6)]	2.808(2)
Ru(3)–Ru(5)	—	—	—	—	2.7568(5)	—	—	—	—
Ru(4)–Ru(5)	—	—	—	—	2.7420(5)	—	—	—	—
Ru(1)–N(1)	2.128(5)	2.123(3)	2.177(7)	2.190(6)	2.164(4)	2.128(8)	2.190(4)	[2.197(4)]	2.25(1)
Ru(2)–N(1)	2.230(5)	2.127(3)	2.178(6)	2.171(5)	2.171(4)	2.214(9)	2.221(4)	[2.135(4)]	2.18(1)
Ru(3)–N(1)	2.173(5)	2.167(3)	2.221(7)	2.177(6)	2.179(4)	2.183(8)	2.148(4)	[2.149(4)]	2.15(1)
Ru(4)–N(1)	2.151(5)	2.235(3)	2.180(6)	2.176(6)	2.167(3)	2.161(8)	2.137(4)	[2.234(4)]	2.16(1)
Ru(1)–C(3)	2.125(6)	2.139(4)	2.113(8)	2.140(7)	2.125(4)	2.089(10)	2.212(5)	[2.216(5)]	2.21(1)
Ru(2)–C(3)	2.384(6)	2.408(3)	2.385(8)	2.46(7)	2.429(4)	2.380(10)	2.339(5)	[2.293(5)]	2.29(1)
Ru(2)–C(4)	2.315(5)	2.311(4)	2.308(8)	2.356(7)	2.303(4)	2.327(10)	2.383(5)	[2.320(5)]	2.35(1)
Ru(3)–C(4)	2.182(6)	2.226(4)	2.175(8)	2.210(7)	2.161(4)	2.19(1)	2.103(5)	[2.108(5)]	2.11(1)
Ru(4)–C(3)	2.421(6)	2.430(4)	2.415(8)	2.376(6)	2.331(4)	2.43(1)	2.293(5)	[2.339(5)]	2.35(1)
Ru(4)–C(4)	2.290(6)	2.384(3)	2.284(8)	2.331(7)	2.317(4)	2.31(1)	2.333(5)	[2.391(5)]	2.37(1)
Ru(1)–P(2)	—	—	—	—	—	—	—	—	2.423(4)
Ru(3)–P(1)	—	—	—	—	—	—	2.355(1)	[2.362(2)]	2.351(4)
Ru(1)–N(2)	—	—	—	—	—	2.10(1)	—	—	—
N(2)–C(17)	—	—	—	—	—	1.12(1)	—	—	—
C(17)–C(18)	—	—	—	—	—	1.47(2)	—	—	—
N(1)–O(1)	1.454(7)	1.451(4)	—	—	—	1.442(10)	1.472(5)	[1.464(5)]	1.42(1)
N(1)–C(2)	—	—	1.41(1)	1.417(9)	—	—	—	—	—
C(2)–O(2)	—	—	1.19(1)	1.185(9)	—	—	—	—	—
C(2)–O(1)	—	—	1.325(10)	1.317(9)	—	—	—	—	—
O(1)–C(1)	1.412(9)	1.404(6)	1.44(1)	1.46(1)	—	1.41(1)	1.390(8)	[1.382(8)]	1.23(2)
N(1)–H	—	—	—	—	1.09	—	—	—	—
C(3)–C(4)	1.400(8)	1.414(5)	1.41(1)	1.402(10)	1.426(6)	1.39(1)	1.423(7)	[1.410(8)]	1.41(2)
Ru(2)–Ru(1)–Ru(4)	82.08(2)	82.36(1)	81.09(3)	82.30(2)	82.55(1)	82.72(4)	84.70(2)	[84.85(2)]	84.16(6)
Ru(1)–Ru(2)–Ru(3)	92.74(2)	94.59(1)	94.42(3)	95.17(3)	97.04(1)	92.83(4)	94.22(2)	[94.85(2)]	95.97(5)
Ru(2)–Ru(3)–Ru(4)	85.16(2)	85.12(1)	83.81(3)	83.76(2)	82.96(1)	85.23(4)	80.27(2)	[80.17(2)]	79.67(5)
Ru(1)–Ru(4)–Ru(3)	94.89(2)	92.95(1)	96.66(3)	94.87(3)	92.88(1)	94.81(4)	95.34(2)	[94.68(2)]	95.72(5)
Ru(3)–Ru(4)–Ru(5)	—	—	—	—	59.93(1)	—	—	—	—
Ru(3)–Ru(5)–Ru(4)	—	—	—	—	60.67(1)	—	—	—	—
Ru(4)–Ru(3)–Ru(5)	—	—	—	—	59.40(1)	—	—	—	—
Ru(1)–N(1)–Ru(2)	80.0(2)	79.9(1)	80.3(2)	77.9(2)	77.0(1)	79.8(3)	75.4(1)	[76.7(1)]	74.4(3)
Ru(1)–N(1)–Ru(4)	79.3(2)	79.6(1)	77.4(2)	77.9(2)	79.2(1)	78.8(3)	76.2(1)	[74.3(1)]	75.0(4)
Ru(2)–N(1)–Ru(3)	75.4(2)	77.3(1)	75.7(2)	76.7(2)	75.4(1)	75.8(3)	80.2(1)	[81.6(2)]	80.7(4)
Ru(3)–N(1)–Ru(4)	76.4(2)	75.35(9)	75.2(2)	76.9(2)	79.4(1)	76.1(3)	81.4(1)	[80.0(1)]	81.2(4)
Ru(1)–N(1)–Ru(3)	135.4(2)	135.9(2)	133.5(3)	133.8(3)	135.1(2)	134.4(4)	137.3(2)	[136.8(2)]	135.6(5)
Ru(2)–N(1)–Ru(4)	112.0(2)	112.8(1)	111.2(3)	112.2(2)	112.3(2)	112.6(4)	112.1(2)	[111.8(2)]	111.7(4)
Ru(1)–C(3)–C(4)	123.2(4)	124.4(3)	123.9(6)	124.1(5)	123.3(3)	124.3(8)	125.1(3)	[125.0(4)]	125.7(10)
Ru(3)–C(4)–C(3)	130.3(4)	127.4(3)	131.7(6)	129.7(5)	130.9(3)	129.7(7)	129.6(4)	[130.0(4)]	130(1)
Ru(1)–N(2)–C(17)	—	—	—	—	—	174(1)	—	—	—

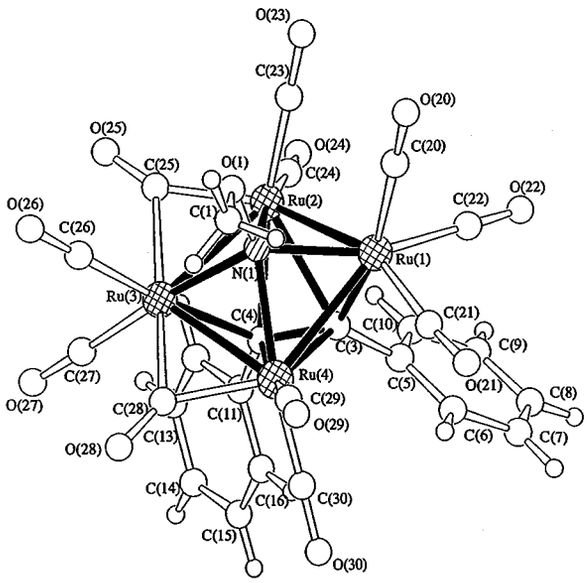

Fig. 2 The molecular structure of $[Ru_4(CO)_9(\mu\text{-}CO)_2(\mu_4\text{-}NOMe)(\mu_4\text{-}\eta^2\text{-}RC_2Ph)]$ illustrated by **3b** (R = Ph); the structure of **3a** (R = H), and its atom numbering scheme, are very similar but with the phenyl ring attached to C(4) replaced by an H atom.

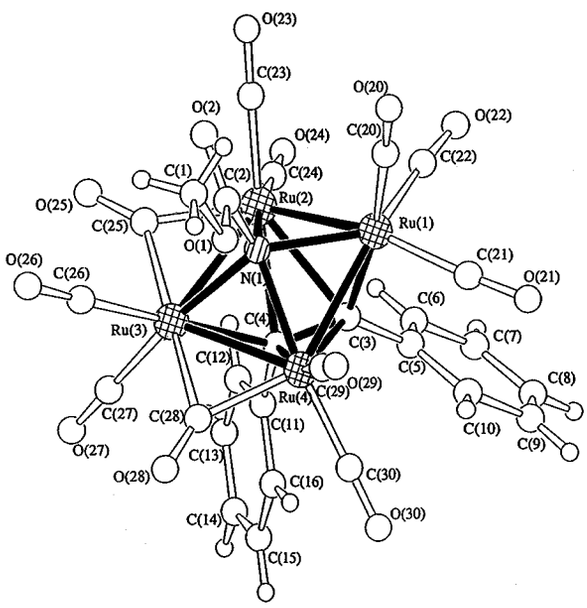

Fig. 3 The molecular structure of $[Ru_4(CO)_9(\mu\text{-}CO)_2\{\mu_4\text{-}NC(O)OMe\}(\mu_4\text{-}\eta^2\text{-}RC_2Ph)]$ illustrated by **4b** (R = Ph); the structure of **4a** (R = H), and its atom numbering scheme, are very similar but with the phenyl ring attached to C(4) replaced by an H atom.

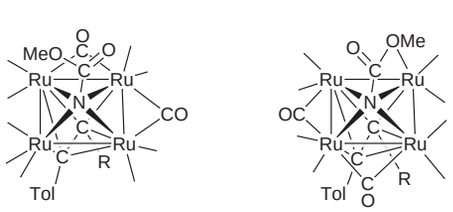

$(\mu\text{-}CO)_2(\mu_4\text{-}S)(\mu_4\text{-}\eta^2\text{-}PhC_2Ph)]$.[8] The acetylenic carbon atoms of phenylacetylene are bonded to three metal atoms. The ligand may be viewed as σ bonded to Ru(1) and Ru(3) and π bonded to Ru(2) and Ru(4). The C–C bond distances in the phenylacetylene ligand [C(3)–C(4) 1.400(8) in **3a** and 1.41(1) Å in **4a**] are not significantly different from that of **2a**. In **3a** and **4a**, μ_4-NOMe and μ_4-NC(O)OMe ligands respectively are situated on the opposite side. The nitrene N atoms symmetrically cap the square bases and lie above the basal plane with a distance to the

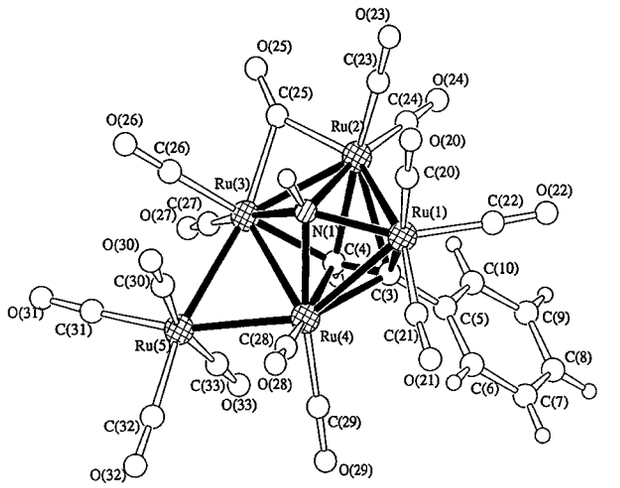

Fig. 4 The molecular structure of $[Ru_5(CO)_{13}(\mu\text{-}CO)(\mu_4\text{-}NH)(\mu_4\text{-}\eta^2\text{-}HC_2Ph)]$ **5a** with the atom numbering scheme.

mean plane of 1.022 and 1.050 Å for **3a** and **4a** respectively. The average Ru–N distances of 2.171(5) for **3a** and 2.189(5) Å for **4a** are slightly longer than those in **2a** [average Ru–N 2.067(7) Å]. The carbamate moiety μ_4-NC(O)OMe in **4a** is essentially coplanar with a maximum deviation of 0.0258 Å. It is mutually perpendicular to the metal plane Ru(1)–Ru(2)–Ru(3)–Ru(4) as the dihedral angle between these two planes is 88.41°. Cluster **4a** is a rare example of a cluster containing a μ_4-NC(O)OMe group. The formation of this ligand seems to involve the cleavage of the bound methoxy moiety while one carbonyl ligand is inserted in between, although the detailed mechanism remains unknown. This kind of CO insertion within the nitrene fragment has also been observed in the pyrolysis reaction of $[Ru_3(CO)_9(\mu\text{-}H)_2(\mu_3\text{-}NOMe)]$.[6a] The molecular structure of **5a** is shown in Fig. 4 and the intramolecular bond distances and angles are listed in Table 3. The metal core of **5a** is similar to those of **3a** and **4a** except that one Ru–Ru bond is now bridged by a $Ru(CO)_4$ group instead of a CO in **3a** or **4a**. This metal framework has been observed in $[Ru_5(CO)_{13}(\mu\text{-}CO)(\mu_4\text{-}S)(\mu_4\text{-}\eta^2\text{-}HC_2Ph)]$.[8] The Ru–Ru distances ranged from 2.6589(5) to 2.7772(5) Å. The square base Ru(1)–Ru(2)–Ru(3)–Ru(4) is slightly distorted with a mean deviation of 0.192 Å, by the quadruply bridging PhC_2H ligand. The plane of Ru(3)–Ru(4)–Ru(5) flaps above this square plane to give a dihedral angle of 166.82° between them. The co-ordination mode of this alkyne moiety towards the square base is the same as that observed in **3a** and **4a** with a C(3)–C(4) distance of 1.426(6) Å. The nitrene N atom caps the tetraruthenium base symmetrically with average Ru–N distance of 2.170(6) Å. The hydrogen atom was located by Fourier-difference synthesis using low angle data at 1.09 Å from the μ_4-nitrene N atom. If the μ_4-NH and the quadruply bridging phenylacetylene group are both assigned to be four-electron donors, a cluster valence electron (CVE) count of 76 results which is consistent with a pentaruthenium cluster with six metal–metal bonds. Nevertheless, the source of the proton in the NH group is uncertain. However we believe that the formation of **5a** involves Ru-assisted cleavage of the bound methoxynitrido moiety.

Pyrolysis of $[Ru_3(CO)_9(\mu_3\text{-}NOMe)(\mu_3\text{-}\eta^2\text{-}HC_2Ph)]$ 2a

Solid state pyrolysis of cluster **2a** at 140 °C for 30 min yields the same products as in the thermolytic reaction, although the distribution is different. Compounds **3a**, **4a** and **5a** were isolated in 19, 26 and 4% yields respectively, whilst $[Ru_3(CO)_{12}]$ (10%), $[Ru_6C(CO)_{17}]$ (6%) and $[Ru_4(CO)_{12}(\mu_4\text{-}\eta^2\text{-}HC_2Ph)]$ (8%) were also obtained through separation by preparative TLC on silica. Cluster **4a** was obtained in a higher yield than **3a** compared to that in the thermolytic reaction. This observation suggests a higher CO pressure may favour the formation of **4a**. However,

3a does not lead to the formation of **4a** upon CO bubbling under ambient conditions.

Thermolysis of $[Ru_3(CO)_9(\mu_3\text{-NOMe})(\mu_3\text{-}\eta^2\text{-}PhC_2Ph)]$ 2b

Cluster **2b** was heated in refluxing *n*-octane until complete consumption was observed by TLC monitoring. Four products identified as $[Ru_4(CO)_9(\mu\text{-}CO)_2(\mu_4\text{-NOMe})(\mu_4\text{-}\eta^2\text{-}PhC_2Ph)]$ **3b**, $[Ru_4(CO)_9(\mu\text{-}CO)_2\{\mu_4\text{-NC(O)OMe}\}(\mu_4\text{-}\eta^2\text{-}PhC_2Ph)]$ **4b**, $[Ru_4(CO)_9(\mu\text{-}CO)_2(\mu_4\text{-NH})(\mu_4\text{-}\eta^2\text{-}PhC_2Ph)]$ **6b** and $[Ru_6(CO)_{13}(\mu\text{-H})(\mu_5\text{-N})(\mu_3\text{-}\eta^2\text{-}PhC_2Ph)_2]$ **7b** were isolated in 18, 10, 12 and 6% yields respectively. Cluster **6b** has been reported elsewhere. According to Blohm and Gladfelter,[4] protonation of $[Ru_4(CO)_{12}(\mu_4\text{-N})]^-$ in the presence of diphenylacetylene gives **6b** as the major product. Spectroscopic data of **6b** including ^{15}N NMR results are given in Table 1 for comparison. A doublet [$J(^{15}NH) = 70.54$ Hz] is observed for the μ_4-NH nitrogen atom in its ^1H coupled ^{15}N NMR spectrum. This ^{15}N–H coupling can be converted into ^{14}N–H coupling by the equation $J(^{14}NH) = -0.713J(^{15}NH)$, where -0.713 comes from γ_{14}/γ_{15}.[12] The $J(^{14}NH)$ observed in the ^1H NMR spectrum of **6b** deviates from the calculated $J(^{14}NH)$ by only 0.83%. The coupling of the ^{15}N NMR signal of **6b** with hydrogen provides strong evidence of the presence of the μ_4-NH proton, which cannot be located easily by X-ray crystallographic studies. The spectroscopic data for **3b**, **4b** and **7b** are summarized in Table 1. For compounds **3b** and **4b** the ^1H NMR spectra consist of singlets at δ 1.78 and 2.96 with an integral of three protons assigned to the μ_4-NOMe and μ_4-NC(O)OMe group protons. A hydride resonance at δ −22.68 is found in the ^1H NMR of **7b** in addition to the signal at δ 7.07 due to the phenyl groups. The mass and IR spectra show that both **3b** and **4b** contain four ruthenium atoms each and both terminal and bridging carbonyls. In contrast, **7b** is a hexaruthenium cluster containing only terminal carbonyls as shown by its mass and IR spectra.

The molecular structures of compounds **3b** and **4b** have been established by single-crystal X-ray analyses and are depicted in Figs. 2 and 3. Selected bond lengths and angles are listed in Table 3. The molecular geometries of **3b** and **4b** are similar to those of **3a** and **4a** respectively, except for the presence of quadruply bridging diphenylacetylene ligands instead of phenylacetylene ligands. Both **3b** and **4b** have an approximate C_s symmetry with the non-crystallographic mirror plane containing the nitrogen atom and two acetylenic carbons. The nitrene N atom in **3b** and **4b** gives a singlet in their corresponding ^{15}N NMR spectra at δ 301.6 and 79.9. The μ_4-NC(O)OMe moiety present in **4b** is essentially planar with a maximum deviation of 0.006 Å and is mutually perpendicular to the metal plane Ru(1)–Ru(2)–Ru(3)–Ru(4) with a dihedral angle of 91.72°.

Dark red crystals of $[Ru_6(CO)_{13}(\mu\text{-H})(\mu_5\text{-N})(\mu_3\text{-}\eta^2\text{-}PhC_2Ph)_2]$ **7b** were grown from a solution of *n*-hexane–dichloromethane by slow evaporation at −20 °C for 3 d. The molecular structure of **7b** is illustrated in Fig. 5 and the relevant bond distances and angles are listed in Table 4. A half molecule of CH_2Cl_2, as the solvent of crystallization, was revealed in the crystal lattice with a twofold positional disorder. The five ruthenium atoms Ru(1), Ru(2), Ru(3), Ru(4) and Ru(5) were arranged in the form of a wingtip-bridged butterfly. An additional $Ru(CO)_2$ group was found to bridge the Ru(4)–Ru(5) edge. This kind of metal skeleton has been observed in $[Ru_6(CO)_{17}(\mu_4\text{-S})_2]$[13] and $[Os_6(CO)_{17}(\mu_4\text{-S})_2]$.[14] Two edges of the wing [Ru(1)–Ru(4) 2.948(3) and Ru(3)–Ru(4) 2.968(3) Å] are significantly longer than the other wing edges [Ru(1)–Ru(2) 2.792(4) and Ru(2)–Ru(3) 2.792(3) Å]. The bridged Ru(4)–Ru(5) [2.677(3) Å] is significantly shorter than the unbridged Ru(2)–Ru(5) [2.935(3) Å], thus the Ru(5) atom is placed slightly towards the Ru(4) atom. Atom Ru(6) caps symmetrically across the Ru(4)–Ru(5) bond with average Ru–Ru distance of 2.668(5) Å. The nitrido nitrogen atom is bonded to five ruthenium atoms of the bridged-butterfly metal framework. This co-ordination mode is rarely observed for the μ_5-nitrido group. Most metal complexes containing a semi-interstitial nitrogen atom have a square-based pyramidal geometry.[15–18] In the complex $[PtRh_{10}N(CO)_{21}]^{3-}$ the interstitial nitrido atom is bonded to 4 Rh and 1 Pt atoms and can be described as having a distorted trigonal bipyramidal environment.[19] This μ_5-N atom in **7b** exhibits an unusually low field signal in the ^{15}N NMR spectrum (δ 549.77) when compared with that of $[Ru_5N(CO)_{16}]^-$ (δ 464.9).[16] In fact this value is rather similar to that of the $[Ru_6N(CO)_{16}]^-$ anion (δ 559.8).[16] The five Ru–N distances range from 1.94(2) to 2.07(2) Å with the nitrido atom displaced towards Ru(4). Two triply bridging diphenylacetylene ligands are co-ordinated on each side of the triruthenium [Ru(4)–Ru(5)–Ru(6)] plane with the acetylenic C(1)–C(2) and C(3)–C(4) bonds lying nearly parallel to the Ru(4)–Ru(5) edge. These alkyne ligands contribute a total of eight electrons to the overall CVE count giving a total of 88 electrons which is consistent with hexaruthenium clusters with nine metal–metal bonds. The hydride ligand revealed by the ^1H NMR spectrum was located by Fourier-difference synthesis and found to bridge the Ru(1)–Ru(3) edge.

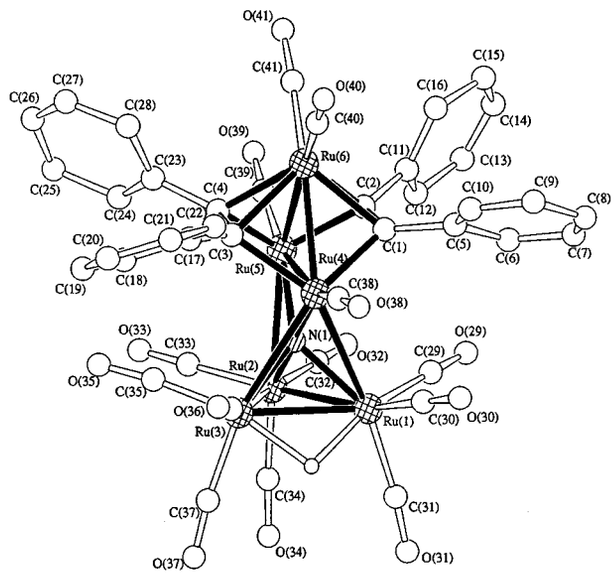

Fig. 5 The molecular structure of $[Ru_6(CO)_{13}(\mu\text{-H})(\mu_5\text{-N})(\mu_3\text{-}\eta^2\text{-}PhC_2Ph)_2]$ **7b** with the atom numbering scheme (hydrogen atoms omitted from phenyl rings of alkyne ligand for clarity).

Table 4 Selected bond lengths (Å) and angles (°) for compound **7b**

Ru(1)–Ru(2)	2.792(4)	Ru(4)–N(1)	1.94(2)
Ru(1)–Ru(3)	2.819(3)	Ru(5)–N(1)	2.02(2)
Ru(1)–Ru(4)	2.948(3)	Ru(4)–C(1)	2.06(3)
Ru(2)–Ru(3)	2.792(3)	Ru(4)–C(3)	2.12(3)
Ru(2)–Ru(5)	2.935(3)	Ru(5)–C(2)	2.00(3)
Ru(3)–Ru(4)	2.968(3)	Ru(5)–C(4)	2.04(3)
Ru(4)–Ru(5)	2.677(3)	Ru(6)–C(1)	2.15(3)
Ru(4)–Ru(6)	2.655(3)	Ru(6)–C(2)	2.12(3)
Ru(5)–Ru(6)	2.680(3)	Ru(6)–C(3)	2.18(3)
Ru(1)–N(1)	2.07(2)	Ru(6)–C(4)	2.13(3)
Ru(2)–N(1)	2.01(2)	C(1)–C(2)	1.39(3)
Ru(3)–N(1)	2.07(2)	C(3)–C(4)	1.44(3)
Ru(2)–Ru(1)–Ru(3)	59.69(9)	Ru(4)–Ru(5)–N(1)	46.3(5)
Ru(1)–Ru(2)–Ru(3)	60.63(8)	Ru(1)–N(1)–Ru(2)	86.3(7)
Ru(1)–Ru(3)–Ru(2)	59.68(9)	Ru(1)–N(1)–Ru(3)	85.7(7)
Ru(3)–Ru(1)–Ru(4)	61.90(8)	Ru(2)–N(1)–Ru(3)	86.1(7)
Ru(1)–Ru(3)–Ru(4)	61.19(8)	Ru(1)–N(1)–Ru(4)	94.5(9)
Ru(1)–Ru(4)–Ru(3)	56.91(8)	Ru(3)–N(1)–Ru(4)	95.2(8)
Ru(2)–Ru(5)–Ru(4)	89.55(9)	Ru(2)–N(1)–Ru(4)	178(1)
Ru(4)–Ru(5)–Ru(6)	59.42(8)	Ru(2)–N(1)–Ru(5)	93.5(1)
Ru(5)–Ru(4)–Ru(6)	60.36(8)	Ru(4)–N(1)–Ru(5)	85.1(7)
Ru(4)–Ru(6)–Ru(5)	60.23(8)	Ru(4)–C(1)–C(2)	106(1)
Ru(5)–Ru(2)–N(1)	43.3(6)	Ru(5)–C(2)–C(1)	110(1)
Ru(5)–Ru(4)–N(1)	48.6(6)	Ru(4)–C(3)–C(4)	104(1)
Ru(2)–Ru(5)–N(1)	43.2(5)	Ru(5)–C(4)–C(3)	109(1)

Reactions of $[Ru_3(CO)_9(\mu_3\text{-}CO)(\mu_3\text{-}NOMe)]$ 1 with alkynes in *n*-octane

Heating cluster **1** with an excess of phenylacetylene in *n*-octane to reflux for 4 h affords a similar product distribution to the thermolytic reaction of **2a** with one new binuclear metallapyrrolidone complex $[Ru_2(CO)_6\{\mu\text{-}\eta^3\text{-}HC_2(Ph)C(O)N(OMe)\}]$ **8a** being isolated in low (3%) yield (Scheme 1). This complex is formed by the combination of the phenylacetylene with CO and the μ_3-NOMe ligand. The spectroscopic data for **8a** are listed in Table 1. The mass and IR spectra show that it is a diruthenium compound with terminal carbonyls only. The 1711 cm^{-1} stretching band observed in the solid-state IR (KBr disc) is assigned to the ketone carbonyl group which is not bound to a metal atom. The three sets of ^1H NMR signals at δ 8.72, 7.72–7.37 and 3.46 are attributed to the acetylenic, phenyl ring and methoxynitrido protons respectively. Unfortunately, the extremely poor yield of **8a** precludes any satisfactory ^{15}N NMR measurements. In order to establish the molecular structure of **8a** the compound has been characterized by X-ray crystallographic analysis (Fig. 6). Selected bond parameters are in Table 5. The molecular geometry of **8a** is similar to that of $[Ru_2(CO)_6\{\mu\text{-}\eta^3\text{-}PhC_2(R)C(O)NPh\}]$ (R = Ph or Me).[2] The two ruthenium atoms are joined by a Ru–Ru single bond [2.6576(3) Å] and bridged by the μ-$HC_2(Ph)$-C(O)N(OMe) ligand. This ligand is similar to that in $[Rh_2Cp_2\{\mu\text{-}CF_3C{=}C(CF_3)C(O)NPh\}]$.[20] However, the synthetic pathway is completely different from that of $[Rh_2Cp_2\{\mu\text{-}CF_3C{=}C(CF_3)C(O)NPh\}]$ which is prepared by the reaction of an alkyne complex with a source of phenylnitrene (such as PhN_3, PhNCO). Although the mechanism of formation of **8a** is uncertain, the compound represents a rare example of the coupling of the μ_3-NOMe ligand with another fragment, CO in this case. The metallocyclic ring system involving Ru(1), N(1), C(2), C(3) and C(4) is essentially planar with the mean deviations from the least-squares plane of 0.137 Å and the Ru(2) atom is found to lie at 1.942 Å from this pentagonal base plane. The nitrogen atom caps the Ru(1)–Ru(2) edge symmetrically with Ru(1)–N(1) 2.108(2) Å and Ru(2)–N(1) 2.132(2) Å. The phenylacetylene ligand adopted a σ,π-vinyl ligand co-ordination mode towards two ruthenium atoms with the unsubstituted carbon C(4) bonded to Ru(1) [2.046(3) Å] and Ru(2) [2.234(3) Å], while the phenyl-substituted carbon C(3) is bonded to Ru(2) [2.293(3) Å] only. Atom C(4) was placed slightly closer to Ru(1) as evident from the Ru(1)–C(4) and Ru(2)–C(4) bond distances, since C(4) is σ bonded to Ru(1) and only π bonded to Ru(2). The C(3)–C(4) distance of the alkyne ligand is typical of π-bonded olefin ligands [1.398(4) Å].

The product distribution of the analogous reaction using diphenylacetylene is similar to that in the thermolytic reaction of **2b**. However, we were unable to isolate the analogous product to **8a** in this case.

Reactivities of complexes 3a and 4a

The reactivities of complexes **3a** and **4a** will be of interest as they are rare examples of clusters containing a μ_4-NOMe and μ_4-NC(O)OMe moiety in which the methoxy and methoxycarbonyl groups seem to be better leaving groups than the phenyl group in a μ_4-NPh nitrene ligand, such as in $[Ru_4(CO)_9(\mu\text{-}CO)_2(\mu_4\text{-}NPh)(\mu_4\text{-}\eta^2\text{-}PhC_2Ph)]$.[5] Besides, **3a** can be prepared in a higher yield than **3b** and it contains an asymmetric alkyne that allows more specific reactivity (Scheme 2).

Thermolysis of 3a in *n*-octane. Heating complex **3a** in refluxing *n*-octane for 4 h gives **4a** as major product along with decomposition of the starting material. Thus **3a** should be an intermediate in the formation of **4a** by Ru-assisted insertion of a CO molecule into the μ_4-NOMe moiety. Owing to the absence of any external CO sources, the CO molecules must come from the degradation of other **3a** molecules. Therefore, significant decomposition of the starting cluster is not unexpected.

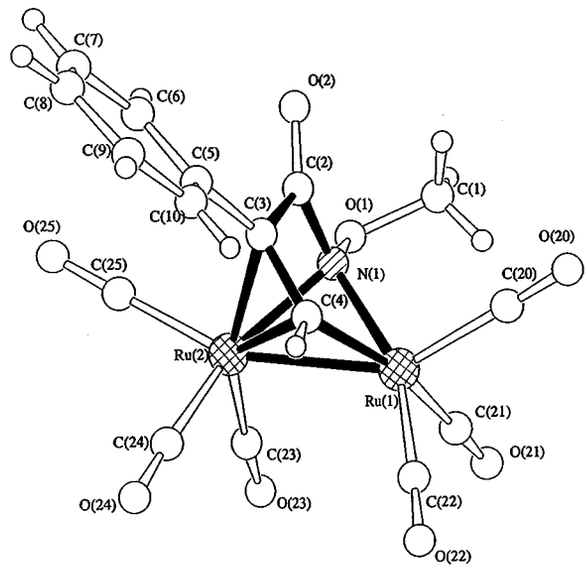

Fig. 6 The molecular structure of $[Ru_2(CO)_6\{\mu\text{-}\eta^3\text{-}HC_2(Ph)C(O)N(OMe)\}]$ **8a** with the atom numbering scheme.

Table 5 Selected bond lengths (Å) and angles (°) for compound **8a**

Ru(1)–Ru(2)	2.6576(3)	N(1)–O(1)	1.418(3)
Ru(1)–N(1)	2.108(2)	N(1)–C(2)	1.423(4)
Ru(2)–N(1)	2.132(2)	C(1)–O(1)	1.424(4)
Ru(1)–C(4)	2.046(3)	C(2)–O(2)	1.199(3)
Ru(2)–C(3)	2.293(3)	C(2)–C(3)	1.499(3)
Ru(2)–C(4)	2.234(3)	C(3)–C(4)	1.398(4)
Ru(1)–Ru(2)–N(1)	50.80(7)	Ru(1)–N(1)–Ru(2)	77.63(8)
Ru(2)–Ru(1)–N(1)	51.58(6)	Ru(1)–N(1)–C(2)	115.5(2)
Ru(1)–Ru(2)–C(4)	48.51(7)	Ru(1)–C(4)–Ru(2)	76.64(9)
Ru(2)–Ru(1)–C(4)	54.86(7)	Ru(1)–C(4)–C(3)	119.1(2)
N(1)–Ru(1)–C(4)	74.51(9)		

Carbonylation of 3a. Carbonylation of compound **3a** in refluxing *n*-hexane or *n*-heptane for 4 h resulted in no visible change in IR and spot TLC monitoring. Even in a CO saturated environment, **3a** will not undergo CO insertion to give **4a** at 90 °C. Thus, the energy barrier for this conversion is quite high. The same reaction was repeated using refluxing *n*-octane as solvent and it took 10 h for completion; **3a** is successfully and almost completely converted into **4a** accompanied by small amounts of $[Ru_3(CO)_{12}]$ and **2a**. Therefore, the use of higher temperature in this carbonyl insertion reaction triggers cluster degradation.

Protonation of 3a. On stirring complex **3a** in acidified acetonitrile for 1 d, the solution changes from yellow to orange. Separation by preparative TLC gave a mixture of orange isomeric products of formula $[Ru_4(CO)_8(\mu\text{-}CO)_2(NCMe)(\mu_4\text{-}NOMe)(\mu_4\text{-}\eta^2\text{-}HC_2Ph)]$ **9a** and **9a′** isolated in 65% yield together with clusters **3a** and **2a** each obtained in 5% yield. Complexes **9a** and **9a′** are air-sensitive and decompose gradually in solution in an inert atmosphere. Their spectroscopic data are presented in Table 1. The IR spectrum of these isomers shows the presence of both terminal and bridging carbonyl ligands. Also the mass spectrum exhibits a molecular ion envelope which agrees with the formulation proposed, with ion peaks corresponding to CO losses. The presence of two isomers of **9a** was evidenced by the ^1H NMR study, two sets of signals in the ratio of about 2:3 (**9a**:**9a′**) being observed. These two isomers are not interconvertible according to a variable temperature ^1H NMR study. The ratio between **9a** and **9a′** is unchanged through −80 to 20 °C. The methyl protons of co-ordinated acetonitrile are found at δ 2.16 and 2.11 for **9a** and **9a′** respectively.

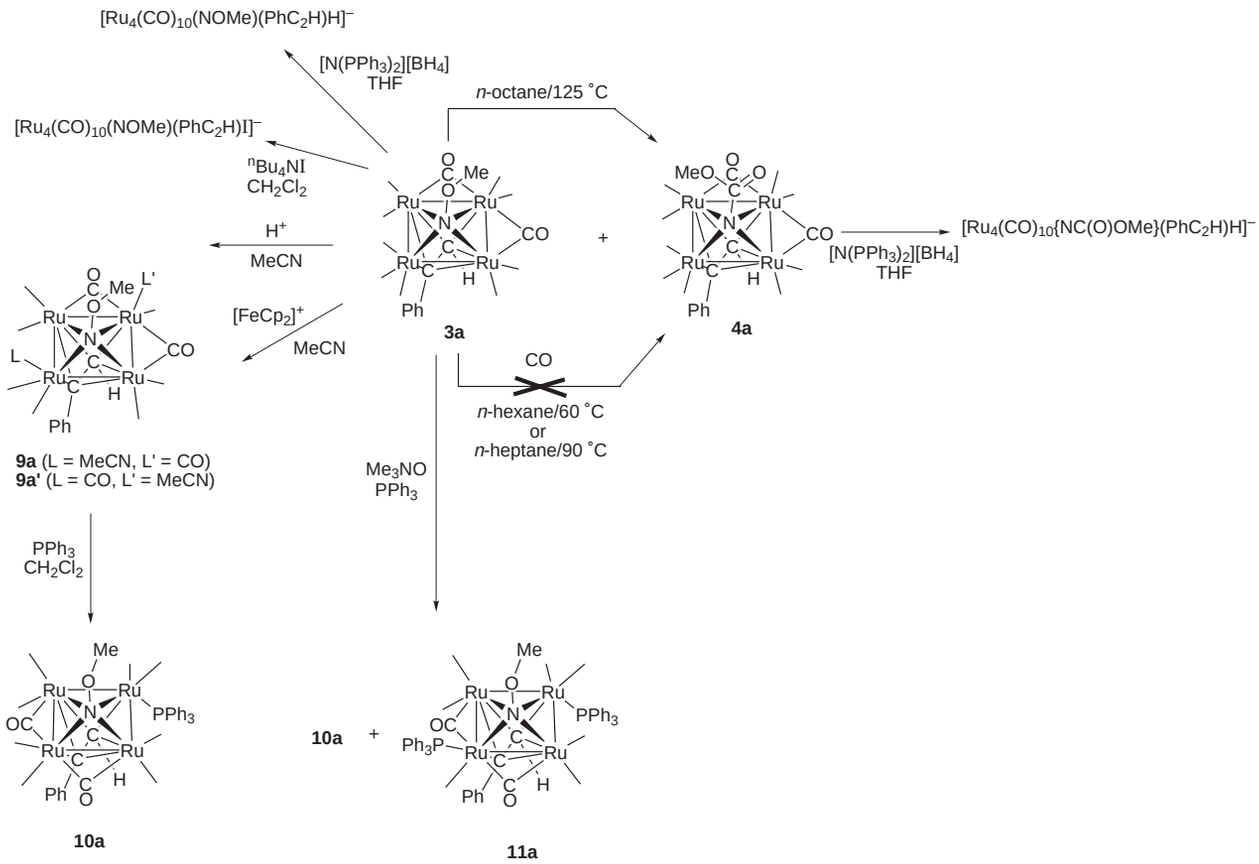

Scheme 2

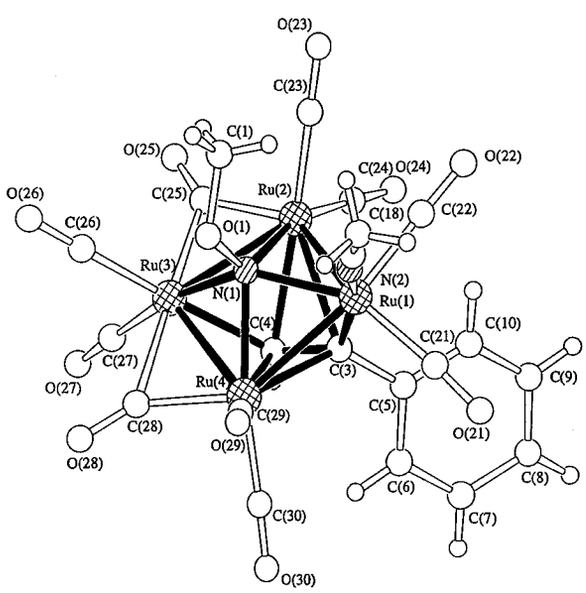

Fig. 7 The molecular structure of $[Ru_4(CO)_8(\mu\text{-}CO)_2(NCMe)(\mu_4\text{-}NOMe)(\mu_4\text{-}\eta^2\text{-}HC_2Ph)]$ **9a** with the atom numbering scheme.

X-Ray quality crystals of cluster **9a** were grown from a CH_2Cl_2–*n*-hexane solution. A perspective view of the molecular structure is shown in Fig. 7. Selected interatomic distances and angles are listed in Table 3. The cluster can be viewed as a monoacetonitrile substituted derivative of **3a**. A terminal CO ligand is removed from the Ru(1) atom in **3a** and replaced by an acetonitrile molecule. The four ruthenium atoms defining the twisted square plane Ru(1)–Ru(2)–Ru(3)–Ru(4) have a mean deviation of 0.188 Å. The Ru–Ru bond lengths in this square base span a range from 2.676(1) to 2.786(1) Å. The two shorter edges correspond to the CO-bridged Ru(2)–Ru(3) and Ru(3)–Ru(4) bonds. One side of the cluster is capped by a quadruply bridging HC_2Ph ligand similar to that in **3a** and **4a**. The other side of the square base contains a μ_4-NOMe ligand which the nitrogen atom caps. The acetonitrile bound to Ru(1) is essentially linear [N(2)–C(17)–C(18) 177(1)°]. Unfortunately, we were unable to obtain single crystals of **9a′** for X-ray analysis, although we suspect that the acetonitrile in **9a′** is co-ordinated to Ru(3) [Ru(1) in **9a**] at the axial position and becomes *trans* to the alkyne ligand based on the similarity in the NMR data of **9a** and **9a′** (Scheme 2).

Oxidation of 3a. When complex **3a** was allowed to react with a slight excess of $[FeCp_2]^+$ in MeCN at room temperature **9a** and **9a′** were isolated in 50% yield along with a small amount of **2a** and **3a**. Significant decomposition of the starting cluster was observed. However, the time required for the completion of reaction is shorter than that when using acidified acetonitrile. Oxidation of **3a** by $[FeCp_2]^+$ facilitates the CO dissociation which is a key step for acetonitrile substitution. Complexes **9a** and **9a′** can be regarded as the activated forms of **3a**. They are very useful for the preparation of derivatives of **3a** with good selectivity.

Substitution on 9a and 9a′. Activated μ_4-NOMe carbonyl clusters **9a** and **9a′** were allowed to react with a stoichiometric amount of triphenylphosphine at room temperature; $[Ru_4(CO)_8(\mu\text{-}CO)_2(PPh_3)(\mu_4\text{-}NOMe)(\mu_4\text{-}\eta^2\text{-}HC_2Ph)]$ **10a** was obtained as orange crystals in 95% yield. The acetonitrile groups in **9a** and **9a′** are shown to be labile and can be replaced by a two-electron donor ligand. Complex **10a** was fully characterized by conventional spectroscopic techniques and elemental analyses (Table 1). The solution IR spectrum in the region 1600–2200 cm^{-1} shows both terminal and bridging carbonyl absorptions. In addition, the mass spectrum of **10a** exhibits the parent ion peak at $m/z = 1093$ with stepwise losses of carbonyls. The ^1H, ^{15}N and ^{31}P NMR signals due to the organic moieties of the complex are fully consistent with its structure and previous

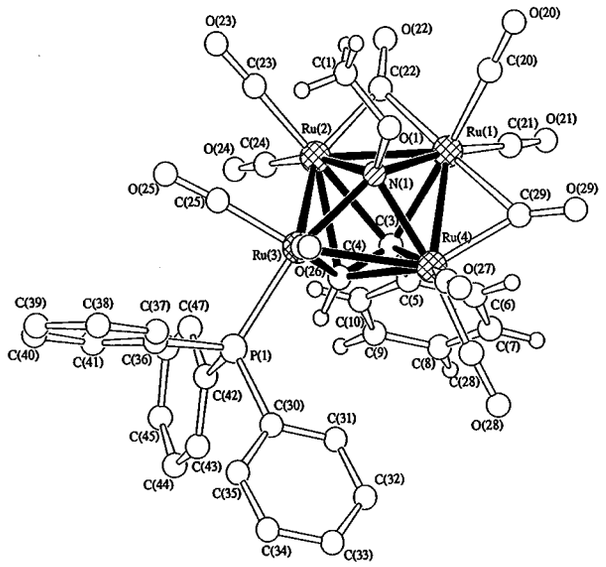

Fig. 8 The molecular structure of $[Ru_4(CO)_8(\mu\text{-}CO)_2(PPh_3)(\mu_4\text{-}NOMe)(\mu_4\text{-}\eta^2\text{-}HC_2Ph)]$ **10a** with the atom numbering scheme (hydrogen atoms omitted from phenyl rings of PPh_3 for clarity).

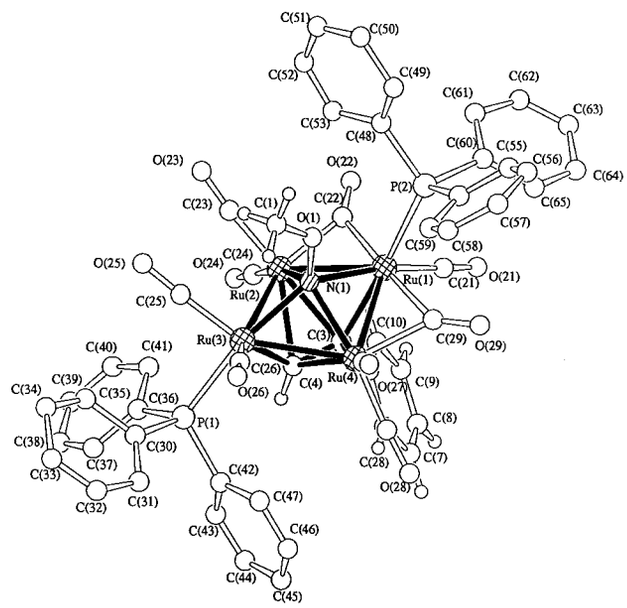

Fig. 9 The molecular structure of $[Ru_4(CO)_7(\mu\text{-}CO)_2(PPh_3)_2(\mu_4\text{-}NOMe)(\mu_4\text{-}\eta^2\text{-}HC_2Ph)]$ **11a** with the atom numbering scheme (hydrogen atoms omitted from phenyl rings of PPh_3 for clarity).

compounds. Signals for the methoxynitrido and phenyl group in the alkyne ligand are all shifted slightly upfield compared with those of **3a** probably because PPh_3 is a poorer π acceptor in comparison to carbonyl. The molecular structure of **10a** has also been established by X-ray crystallography. There are two independent molecules in each asymmetric unit, which are essentially the same differing only by a slight rotation of the μ_4-NOMe and phenyl group of the alkyne moieties. One of the molecules is depicted in Fig. 8, together with the atomic numbering scheme. Selected interatomic distances and angles are given in Table 3. The four ruthenium atoms form a square base arrangement with a quadruply bridging PhC_2H ligand, which is nearly planar with a mean deviation from the least squares plane of 0.210 Å for both Ru(1)–Ru(2)–Ru(3)–Ru(4) and Ru(5)–Ru(6)–Ru(7)–Ru(8). The PPh_3 ligands are substituted at the Ru(3) centre. It occupies a pseudo equatorial position to minimize the steric interaction with other ligands. The transformation from **9a** and **9a′** to **10a** involves dissociation of labile NCMe, rearrangement of CO ligands, co-ordination of PPh_3 and finally rotation down to the site *trans* to the nitrene moiety. The sterically less demanding acetonitrile molecule favours the *trans* position to the alkyne ligand while bulky triphenylphosphine favours an equatorial position that is far away from the μ_4-NOMe and phenyl group of the alkyne. This is because the site of co-ordination by acetonitrile is largely determined by the *trans* influence, while for the bulky phosphine ligand the steric effect becomes important.

Substitution on 3a. Dropwise addition of 1.1 equivalents of Me_3NO to a mixture of cluster **3a** and PPh_3 in CH_2Cl_2 gives **10a** and $[Ru_4(CO)_7(\mu\text{-}CO)_2(PPh_3)_2(\mu_4\text{-}NOMe)(\mu_4\text{-}\eta^2\text{-}HC_2Ph)]$ **11a** in 30 and 20% yields, respectively. Compound **11a** was also characterized by various spectroscopic methods (Table 1). Using the oxygen-transfer reagent, Me_3NO leads to a less selective substitution reaction. Upon further co-ordination of one more PPh_3 ligand the resonance signals for the methoxynitrido and phenyl group protons in the alkyne ligand are further shifted to lower chemical shift values compared to those of **3a** and **10a**. Coupling between the two phosphorus atoms is observed with $J_{PP} = 6.96$ Hz in the ^{31}P NMR spectrum of **11a**. The molecular structure of **11a** is revealed in Fig. 9. Selected intramolecular bond distances and angles are listed in Table 3. One molecule of CH_2Cl_2, as a solvent of crystallization, is found in the crystal lattice. The molecular geometry of compound **11a** is very similar to that of **10a** except that one of the terminal CO ligands on Ru(1) of **10a** is replaced by a PPh_3 ligand. Substitution of either CO will generate unfavourable steric interaction with the μ_4-NOMe or the phenyl ring on the alkyne ligand. It appears that such interaction is less severe with the μ_4-NOMe group. In the structures of **10a** and **11a** the capping sites of bridging carbonyls are opposite to those of the previous ones, which are attached to the same Ru atom [Ru(1)] as C(3).

Reaction of 3a towards iodine and iodide. Compound **3a** decomposes in a CH_2Cl_2 solution in the presence of an excess of iodine, while it reacts with $^nBu_4NI$ to give a new orange compound quantitatively. The cluster was allowed to react with the iodide salt in refluxing CH_2Cl_2 for 3 h. The solvent was removed *in vacuo* and an orange precipitate was left behind after extraction of any starting cluster by *n*-hexane. The negative FAB mass spectrum exhibits a molecular peak envelope at *m*/*z* 958 which is consistent with the proposed formulation of $[Ru_4(CO)_{10}(NOMe)(HC_2Ph)I]^-$ based on the isotopic distribution of the peak.

Reaction of 3a towards hydride. Complex **3a** was allowed to react with $[N(PPh_3)_2][BH_4]$ in refluxing THF for 3 h. The reaction mixture changed from yellow to orange. After removing the solvent *in vacuo*, *n*-hexane was used to extract any starting material. The product shows a peak envelope centred at *m*/*z* 804 with stepwise losses of nine carbonyls in its negative FAB mass spectrum. It is believed that the attack of the hydride ion on **3a** results in the replacement of a carbonyl with a hydride ligand to give a compound with the formula $[Ru_4(CO)_{10}(NOMe)(HC_2Ph)H]^-$. The observed peak at *m*/*z* 804 should correspond to the $[M - CO]^-$ ion. A very similar reaction between **4a** and $[N(PPh_3)_2][BH_4]$ has been observed in which the molecular ion with 10 CO can be detected in the corresponding mass spectrum. The products are air-sensitive and decompose in air in a few minutes; further characterization is thus hindered.

Attempted hydrogenation on 3a. Compound **3a** was hydrogenated in refluxing *n*-hexane, monitored by IR and TLC. However, no reaction was observed after 4 h. Therefore, thermolysis, protonation, hydride attack and hydrogenation all fail to result in the formation of μ_4-NH from a μ_4-NOMe moiety. The mechanism of the formation of the μ_4-NH nitrene cluster is not clear and the μ_4-NOMe cluster should not be an intermediate in the formation of μ_4-NH clusters.

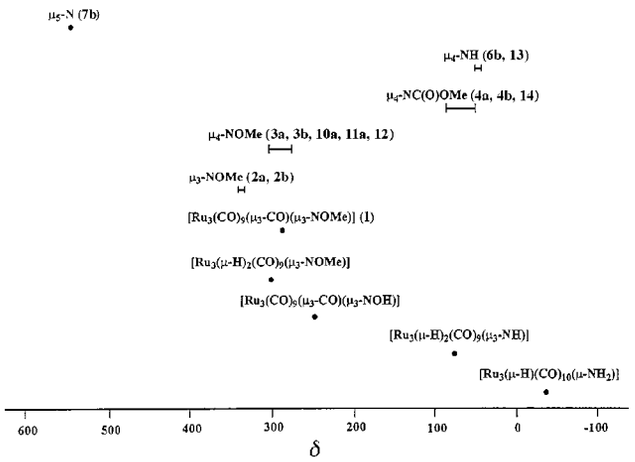

Fig. 10 Summary of the nitrogen chemical shifts for compounds in this study.

^{15}N NMR Spectroscopy

Nitrogen-15 magnetic resonance spectroscopy of metal nitrenes has been little studied. Only a few nitrene and imido ruthenium carbonyl clusters have undergone ^{15}N NMR investigations. They are **1**[21] its hydrido-derivative $[Ru_3(\mu\text{-}H)_2(CO)_9(\mu_3\text{-}NOMe)]$,[22] $[Ru_3(CO)_9(\mu_3\text{-}CO)(\mu_3\text{-}NOH)]$,[23] $[Ru_3(\mu\text{-}H)_2(CO)_9(\mu_3\text{-}NH)]$[22] and $[Ru_3(\mu\text{-}H)(CO)_{10}(\mu\text{-}NH_2)]$.[22] In order to investigate the environment of the different nitrogen atoms of the compounds in this study, ^{15}N NMR studies were performed on clusters **1**–**4**, **6b**, **7b**, **10a** and **11a**. All these data are summarized in Fig. 10; for comparison, compounds $[Ru_4(CO)_9(\mu\text{-}CO)_2(\mu_4\text{-}NOMe)(\mu_4\text{-}\eta^2\text{-}HC_2Tol)]$ **12** (tol = *p*-tolyl), $[Ru_4(CO)_9(\mu\text{-}CO)_2(\mu_4\text{-}NH)(\mu_4\text{-}\eta^2\text{-}HC_2Tol)]$ **13** and $[Ru_4(CO)_9(\mu\text{-}CO)_2\{\mu_4\text{-}NC(O)OMe\}(\mu_4\text{-}\eta^2\text{-}HC_2Tol)]$ **14** which have been reported[7] previously are also listed in Table 1 and Fig. 10.

Clusters **1** and $[Ru_3(CO)_9(\mu_3\text{-}CO)(\mu_3\text{-}NOH)]$ are formed by reactions of $[Ru_3(CO)_{10}(\mu\text{-}NO)]^-$ with $CF_3SO_3CH_3$ and CF_3SO_3H respectively. Their ^{15}N NMR spectra exhibit resonances at δ 287.3 and 250.6[21,23] (reference: liquid NH_3), which are at much lower frequencies than the resonance of $[Ru_3(CO)_{10}(\mu\text{-}NO)]^-$ (δ 814.4).[24] The shift in the nitrogen resonance in going from the μ-NO to μ_3-NOMe or μ_3-NOH is substantially larger in magnitude and in the opposite direction from that observed for the unique carbon resonance when converting $[FeH(CO)_{13}]^-$ into $[Fe_4H(CO)_{12}(COMe)]$ or $[Fe_4H(CO)_{12}(COH)]$.[25] However, in contrast to the carbon system, the μ_3-NOMe resonance is further downfield than that of the μ_3-NOH group. Upon hydrogenation of **1** the $[Ru_3(\mu\text{-}H)_2(CO)_9(\mu_3\text{-}NOMe)]$ formed gives a ^{15}N chemical shift at δ 301.0.[22] Herein, clusters **2a** and **2b** containing the μ_3-NOMe moiety and triply bridging alkynes show resonances at δ 345.9 and 341.5 respectively. Both nitrogen atoms have a more downfield signal compared to that of the starting cluster **1**. Clusters with a μ_4-NOMe ligand and quadruply bridging phenylacetylene (**3a**), diphenylacetylene (**3b**) or tolylacetylene (**12**) ligand exhibit singlets at δ 308.0, 301.6 and 308.3 respectively. Upon further co-ordination of a ruthenium atom there is a roughly 39 ppm upfield shift. Interestingly, the insertion of CO within the nitrene fragment will displace the nitrogen resonance to a higher field by an average of 233 ppm relative to the corresponding μ_4-NOMe clusters. Similar effects were obtained for clusters with the μ_4-NH moiety. Clusters **6b** and **13** give doublets at δ 47.6 [$J(^{15}NH) = 70.5$] and 53.1 [$J(^{15}NH) = 70.6$ Hz] which are also significantly upfield (254.6 ppm) from the respective μ_4-NOMe clusters **3b** and **12**. These observed $J(^{15}NH)$ coupling constants are fully consistent with calculated values. This is the first time that the nitrogen resonance of the μ_4-NH moiety in low-valent clusters has been reported, while the data for the μ_3-NH cluster, $[Ru_3(\mu\text{-}H)_2(CO)_9(\mu_3\text{-}NH)]$, and μ-$NH_2$ cluster, $[Ru_3(\mu\text{-}H)(CO)_{10}(\mu\text{-}NH_2)]$, have been reported elsewhere.[22] The ^{15}N NMR spectrum of $[Ru_3(\mu\text{-}H)_2(CO)_9(\mu_3\text{-}NH)]$ exhibits an absorbance at δ 82.5 downfield from liquid NH_3; $J(^{15}NH) = 77.5$ Hz is characteristic of a direct N–H bond. In the ^{15}N NMR spectrum of $[Ru_3(\mu\text{-}H)(CO)_{10}(\mu\text{-}NH_2)]$ the resonance is centred at δ −33.5 relative to NH_3 which exhibits coupling of all three hydrogen atoms in the molecule. The directly bound N–H coupling constants are 72.7 and 70.9 Hz, and the two-bond coupling constant to the hydride ligand is 2.5 Hz. The chemical shift of μ_4-NH is in between those of μ_3-NH and μ-NH_2, but does not fall on their smooth trend. This effect may be attributed to different degrees of interaction of the nitrogen atom with metals in μ_4-NH when compared to μ_3-NH and μ-NH_2. Substitution of a carbonyl ligand with a PPh_3 ligand on **3a** (δ 308.0) causes an upfield shift of the nitrogen resonance by 27.4 ppm, whilst upon further replacement of one more carbonyl ligand the chemical shift is located at δ 291.3. The first PPh_3 is substituted at an equatorial position *trans* to the nitrene moiety, and the other one is placed at an axial position *trans* to the alkyne ligand. The co-ordination mode of the μ_5-nitrido group in **7b** is rather rare. The five ruthenium atoms form a bridged-butterfly metal skeleton. The μ_5-N atom exhibits an unusual high frequency signal (δ 549.8) in comparison to that of the semi-interstitial nitrogen atom in $[Ru_5N(CO)_{14}]^-$ (δ 464.9).[16] By contrast, this value is rather similar to that of a completely encapulsated environment such as in the $[Ru_6N(CO)_{16}]^-$ anion (δ 559.4).[16] Even on protonation of these anions, an upfield shift of 27–30 ppm is proposed to be observed.[26] Details of the quantitative correlation of the nuclear magnetic deshielding of the nitrogen atom in **7b** with its compression in the cluster are under investigation.

Conclusion

One finding of this study is the large diversity of products that result from the reactions of the triruthenium nitrene clusters with alkynes. Also remarkable is the lack of correspondence between the reactions of alkynes with the analogous $[Ru_3(CO)_9(\mu_3\text{-}CO)(\mu_3\text{-}NPh)]$ cluster.[2] We have demonstrated a viable high-yield route to the representative clusters **2a** and **2b**. The isolation of $[Ru_3(CO)_9(\mu_3\text{-}NOMe)(\mu_3\text{-}\eta^2\text{-}RC_2Ph)]$ (R = H or Ph) in high yields has afforded us an opportunity to study their reactivities in detail. Decarbonylation of such clusters initiates the formation of μ_4-nitrene clusters with alkynes which are believed to be an important moiety to stabilize the Ru_4 skeleton. Clusters containing μ_4-NOMe and μ_4-NC(O)OMe moieties are particularly attractive models for CO insertion in the nitrene ligand. For clusters with a μ_4-NH moiety the origin of the imido hydrogen atom is unclear, with possible sources including abstraction of hydrogen from solvent and/or adventitious water. However, the ^{15}N NMR studies of these clusters give valuable information regarding the environment of the μ_4-NH nitrogen atom.

Experimental

All reactions and manipulations were carried out under argon using standard Schlenk techniques, except for the chromatographic separations. Solvents were purified by standard procedures and distilled prior to use. All chemicals, unless otherwise stated, were purchased commercially and used as received; $[Ru_3(CO)_9(\mu_3\text{-}CO)(\mu_3\text{-}NOMe)]$,[21] $[N(PPh_3)_2][^{15}NO_2]$[24] and $[FeCp_2][PF_6]$[27] were prepared by the literature methods. Reactions were monitored by analytical thin-layer chromatography (Merck Kieselgel 60 F_{254}) and the products were separated by thin-layer chromatography on plates coated with silica (Merck Kieselgel 60 GF_{254}). Infrared spectra were recorded on a Bio-Rad FTS-7 IR spectrometer, using 0.5 mm calcium fluoride solution cells, ^{1}H NMR spectra on a Bruker DPX300 spectrometer using CD_2Cl_2 and referenced to $SiMe_4$ (δ 0), ^{15}N and ^{31}P NMR spectra on a Bruker DPX500

spectrometer using $CDCl_3$ solvent with liquid NH_3 and 85% H_3PO_4 respectively as references. Positive and negative ionization fast atom bombardment (FAB) mass spectra were recorded on a Finnigan MAT 95 mass spectrometer, using *m*-nitrobenzyl alcohol or α-thioglycerol as matrix solvents. Microanalyses were performed by Butterworth Laboratories, UK.

Preparation of $[Ru_3(CO)_9(\mu_3\text{-NOMe})(\mu_3\text{-}\eta^2\text{-}HC_2Ph)]$ 2a

A solution of $[Ru_3(CO)_9(\mu_3\text{-CO})(\mu_3\text{-NOMe})]$ **1** (200 mg, 0.32 mmol) in *n*-hexane (40 ml) was heated with 3 drops of phenylacetylene under an argon atmosphere. The initial yellow solution changed to brown upon refluxing. After 1 h, the solvent was removed under reduced pressure. The residue was redissolved in CH_2Cl_2 (2 ml) and separated by preparative TLC using the eluent *n*-hexane–CH_2Cl_2 (9 : 1, v/v) to afford one yellow band **2a** (R_f 0.75) in 75% yield (168 mg, 0.24 mmol) (Found: C, 30.9; H, 1.4; N, 1.8. Calc. for $C_{18}H_9NO_{10}Ru_3$: C, 30.78; H, 1.29; N, 1.99%).

Preparation of $[Ru_3(CO)_9(\mu_3\text{-NOMe})(\mu_3\text{-}\eta^2\text{-}PhC_2Ph)]$ 2b

A solution of cluster **1** (200 mg, 0.32 mmol) and diphenylacetylene (62 mg, 0.35 mmol) in *n*-hexane was allowed to heat at 60 °C for 1 h, the solvent was then removed *in vacuo* and the residue subjected to TLC using *n*-hexane–CH_2Cl_2 (6 : 1, v/v) as eluent. An intense yellow band $[Ru_3(CO)_9(\mu_3\text{-NOMe})(\mu_3\text{-}\eta^2\text{-}PhC_2Ph)]$ **2b** was isolated in 70% yield (R_f 0.7, 173 mg, 0.22 mmol) (Found: C, 37.1; H, 1.8; N, 1.6. Calc. for $C_{24}H_{13}NO_{10}Ru_3$: C, 37.02; H, 1.68; N, 1.80%).

Thermolysis of compound 2a

Compound **2a** (200 mg, 0.28 mmol) was dissolved in *n*-octane (40 ml). The bright yellow solution was heated at 125 °C for 3 h. The solvent was then removed *in vacuo* and the residue chromatographed on TLC plates using *n*-hexane–CH_2Cl_2 (3 : 1, v/v) as eluent. The first red band was $[Ru_4(CO)_{12}(\mu_4\text{-}\eta^2\text{-}HC_2Ph)]$[10] ($R_f$ 0.85, 9.0 mg, 0.011 mmol, 5%). Three products were isolated in the following order of elution $[Ru_4(CO)_9(\mu\text{-CO})_2(\mu_4\text{-NOMe})(\mu_4\text{-}\eta^2\text{-}HC_2Ph)]$ **3a** (R_f 0.7, 45.9 mg, 0.053 mmol, 25%), $[Ru_5(CO)_{13}(\mu\text{-CO})(\mu_4\text{-NH})(\mu_4\text{-}\eta^2\text{-}HC_2Ph)]$ **5a** (R_f 0.5, 4.8 mg, 0.0047 mmol, 3%) and $[Ru_4(CO)_9(\mu\text{-CO})_2\{\mu_4\text{-NC(O)OMe}\}(\mu_4\text{-}\eta^2\text{-}HC_2Ph)]$ **4a** (R_f 0.45, 28.4 mg, 0.032 mmol, 15%) (Found: C, 27.7; H, 0.9; N, 1.6. Calc. for $C_{20}H_9NO_{12}Ru_4$ **3a**: C, 27.9; H, 1.06; N, 1.63. Found: C, 26.2; H, 0.9; N, 1.5. Calc. for $C_{22}H_7NO_{14}Ru_5$ **5a**: C, 26.04; H, 0.70; N, 1.38. Found: C, 28.6; H, 1.2; N, 1.4. Calc. for $C_{21}H_9NO_{13}Ru_4$ **4a**: C, 28.42; H, 1.02; N, 1.58%).

Pyrolysis of $[Ru_3(CO)_9(\mu_3\text{-NOMe})(\mu_3\text{-}\eta^2\text{-}HC_2Ph)]$ 2a

Compound **2a** (200 mg, 0.28 mmol) was sealed in a Carius tube under reduced pressure and placed in an oven at 140 °C for half an hour. The dark brown residue was then extracted with dichloromethane until the extract became colourless. The solvent was removed and the residue chromatographed on silica gel plates using *n*-hexane–dichloromethane (3 : 1, v/v) as eluent. The first few compounds eluted were $[Ru_3(CO)_{12}]$ (R_f 0.95, 18.2 mg, 0.028 mmol, 10%), $[Ru_4(CO)_{12}(\mu_4\text{-}\eta^2\text{-}HC_2Ph)]$[10] ($R_f$ 0.85, 14.4 mg, 0.017 mmol, 8%) and $[Ru_6C(CO)_{17}]$ (R_f 0.8, 9.4 mg, 0.0085 mmol, 6%). The following compounds **3a**, **4a** and **5a** were isolated in 19 (34.9 mg, 0.041 mmol), 26 (49.3 mg, 0.055 mmol) and 4% (6.9 mg, 0.0068 mmol) yields, respectively.

Thermolysis of compound 2b

A solution of compound **2b** (200 mg, 0.26 mmol) in *n*-octane (40 ml) was refluxed under an argon atmosphere for 3 h. The solution gradually turned from yellow to dark brown. The solvent was removed under reduced pressure. Chromatography on silica with *n*-hexane–dichloromethane (4 : 1, v/v) afforded four bands. Four consecutive bands were then eluted, namely $[Ru_4(CO)_9(\mu\text{-CO})_2(\mu_4\text{-NOMe})(\mu_4\text{-}\eta^2\text{-}PhC_2Ph)]$ **3b** (R_f 0.75, 32.4 mg, 0.035 mmol, 18%), $[Ru_6(CO)_{13}(\mu\text{-H})(\mu_5\text{-N})(\mu_3\text{-}\eta^2\text{-}PhC_2Ph)_2]$ **7b** (R_f 0.7, 10.3 mg, 0.0077 mmol, 6%), $[Ru_4(CO)_9(\mu\text{-CO})_2\{\mu_4\text{-NC(O)OMe}\}(\mu_4\text{-}\eta^2\text{-}PhC_2Ph)]$ **4b** (R_f 0.48, 18.6 mg, 0.019 mmol, 10%) and $[Ru_4(CO)_9(\mu\text{-CO})_2(\mu_4\text{-NH})(\mu_4\text{-}\eta^2\text{-}PhC_2Ph)]$ **6b**[4] (R_f 0.45, 20.9 mg, 0.023 mmol, 12%) (Found: C, 33.5; H, 1.2; N, 1.6. Calc. for $C_{26}H_{13}NO_{12}Ru_4$ **3b**: C, 33.38; H, 1.40; N, 1.50. Found: C, 36.8; H, 1.7; N, 1.2. Calc. for $C_{41}H_{21}NO_{13}Ru_6$ **7b**: C, 36.69; H, 1.58; N, 1.04. Found: C, 33.8; H, 1.5; N, 1.3. Calc. for $C_{27}H_{13}NO_{13}Ru_4$ **4b**: C, 33.65; H, 1.36; N, 1.45%).

Reaction of complex 1 with phenylacetylene in *n*-octane

A suspension of compound **1** (200 mg, 0.32 mmol) in *n*-octane (60 ml) was refluxed with 3 drops of phenylacetylene under an argon atmosphere. The solution gradually changed from yellow to dark brown. Thermolysis was continued until no starting materials remained (about 4 h, as confirmed by IR spectroscopy). The mixture was dried *in vacuo*. The dark brown residue was redissolved in CH_2Cl_2 (2 ml) and TLC separation (*n*-hexane–dichloromethane, 3 : 1, v/v) afforded $[Ru_4(CO)_{12}(\mu_4\text{-}\eta^2\text{-}HC_2Ph)]$[10] ($R_f$ 0.85, 8.0 mg, 0.010 mmol, 4%), **3a** (R_f 0.7, 51.3 mg, 0.060 mmol, 25%), **5a** (R_f 0.5, 5.4 mg, 0.005 mmol, 3%), **4a** (R_f 0.45, 36.0 mg, 0.041 mmol, 17%) and $[Ru_2(CO)_6\{\mu\text{-}\eta^3\text{-}HC_2(Ph)C(O)N(OMe)\}]$ **8a** (R_f 0.2, 7.8 mg, 0.014 mmol, 3%) (Found: C, 33.1; H, 1.8; N, 2.4. Calc. for $C_{16}H_9NO_8Ru_2$ **8a**: C, 33.24; H, 1.66; N, 2.57%).

Thermolysis of complex 3a

Compound **3a** (20 mg, 0.023 mmol) was dissolved in *n*-octane (30 ml). The yellow solution was heated at 125 °C for 4 h which resulted in the formation of a deep brown solution. The solvent was removed under reduced pressure and the only product isolated by TLC, using *n*-hexane–dichloromethane (3 : 1, v/v) as eluent, was **4a** (R_f 0.45, 6.2 mg, 0.007 mmol, 30%) accompanied by a small amount of unchanged **3a** (R_f 0.7, 1.6 mg, 0.0019 mmol, 8%).

Carbonylation of complex 3a in *n*-hexane or *n*-heptane

Compound **3a** (20 mg, 0.023 mmol) was dissolved in *n*-hexane or *n*-heptane (30 ml). The bright yellow solution was heated while CO gas was bubbled through it. Using IR spectroscopic monitoring, no visible change was observed after 4 h.

Carbonylation of complex 3a in *n*-octane

Compound **3a** (20 mg, 0.023 mmol) was dissolved in *n*-octane (30 ml). The yellow solution was then carbonylated under reflux. The reaction was monitored by spot TLC until complete consumption of **3a** (about 10 h). The mixture was dried *in vacuo* and the residue chromatographed on TLC plates using *n*-hexane–dichloromethane (6 : 1, v/v) as eluent. The first band obtained was $[Ru_3(CO)_{12}]$ (R_f 0.9, 5.0 mg, 0.008 mmol, 25%). Compounds **2a** (R_f 0.8, 6.5 mg, 0.009 mmol) and **4a** (R_f 0.65, 6.2 mg, 0.007 mmol) were eluted in sequence with 30% yield of each.

Protonation of complex 3a

Compound **3a** (50 mg, 0.058 mmol) was stirred in acidified acetonitrile (50 ml) prepared by the addition of 0.4 ml of 0.18 M (in MeCN) H_2SO_4 solution to 50 ml of distilled acetonitrile solvent. The reaction was monitored by spot TLC until all starting material had been consumed (about 1 d). The solvent was removed under reduced pressure and the residue chromatographed on silica using *n*-hexane–dichloromethane (3 : 1, v/v) as eluent. The first two yellow bands were found to be **2a** (R_f 0.78, 2.7 mg, 0.004 mmol, 5%) and **3a** (R_f 0.7, 2.5 mg, 0.003 mmol, 5%). The following product **9a** was isolated in 65% yield (R_f 0.3,

Table 6 Crystal data and data collection parameters for compounds **2**–**5a** and **7b**–**11a**

	2a	**2b**	**3a**	**3b**	**4a**	**4b**	**5a**	**7b**	**8a**	**9a**	**10a**	**11a**
Empirical formula	$C_{18}H_9NO_{10}Ru_3$	$C_{24}H_{13}NO_{10}Ru_3$	$C_{20}H_9NO_{12}Ru_4$	$C_{26}H_{13}NO_{12}Ru_4$	$C_{21}H_9NO_{13}Ru_4$	$C_{27}H_{13}NO_{13}Ru_4$	$C_{22}H_7NO_{14}Ru_5$	$C_{41}H_{21}NO_{13}Ru_6{\cdot}0.5CH_2Cl_2$	$C_{16}H_9NO_8Ru_2$	$C_{21}H_{12}N_2O_{11}Ru_4$	$C_{37}H_{24}NO_{11}PRu_4$	$C_{54}H_{39}NO_{10}P_2Ru_4{\cdot}CH_2Cl_2$
M	702.48	778.58	859.57	935.67	887.58	963.68	1014.65	1384.50	545.39	872.61	1093.85	1413.06
Crystal colour, habit	Yellow, block	Yellow, rod	Orange, block	Orange, block	Orange, plate	Orange, block	Blue, block	Red, block	Yellow, block	Orange, plate	Orange, block	Orange, block
Crystal dimensions/mm	0.22 × 0.29 × 0.40	0.24 × 0.13 × 0.12	0.09 × 0.12 × 0.17	0.12 × 0.14 × 0.22	0.07 × 0.24 × 0.34	0.19 × 0.21 × 0.24	0.11 × 0.16 × 0.19	0.13 × 0.13 × 0.33	0.21 × 0.22 × 0.25	0.12 × 0.14 × 0.18	0.22 × 0.22 × 0.24	0.23 × 0.33 × 0.34
Crystal system	Triclinic	Monoclinic	Triclinic	Triclinic	Monoclinic	Triclinic	Triclinic	Triclinic	Monoclinic	Monoclinic	Triclinic	Monoclinic
Space group	$P\bar{1}$ (no. 2)	$P2_1/n$ (no. 14)	$P\bar{1}$ (no. 2)	$P\bar{1}$ (no. 2)	$P2_1/c$ (no. 14)	$P\bar{1}$ (no. 2)	$P\bar{1}$ (no. 2)	$P\bar{1}$ (no. 2)	$P2_1/a$ (no. 14)	$P2_1/c$ (no. 14)	$P\bar{1}$ (no. 2)	$P2_1$ (no. 4)
a/Å	9.603(2)	15.116(2)	9.979(1)	9.984(1)	9.372(1)	9.414(1)	8.964(1)	10.696(1)	13.054(1)	10.136(4)	11.217(1)	11.704(1)
b/Å	16.065(5)	11.029(1)	10.569(1)	10.527(1)	16.092(1)	9.647(1)	12.961(1)	12.118(1)	7.738(1)	16.940(6)	18.763(2)	19.428(2)
c/Å	8.226(3)	17.732(2)	12.611(1)	15.036(1)	18.232(2)	17.936(1)	13.140(1)	17.873(2)	19.384(2)	15.420(5)	20.022(2)	11.915(1)
α/°	101.68(3)		81.35(1)	82.27(1)		84.53(2)	105.22(2)	83.79(1)			98.07(1)	
β/°	112.45(2)	113.01(2)	82.21(2)	72.29(1)	104.20(2)	86.42(2)	104.05(2)	88.44(2)	110.97(2)	92.34(3)	106.28(2)	92.94(1)
γ/°	85.58(2)		80.71(1)	75.44(1)		69.85(2)	91.33(1)	74.11(2)			102.58(2)	
U/Å^3	1148.6(6)	2721.0(7)	1289.2(2)	1454.2(3)	2665.6(5)	1521.5(3)	1420.0(3)	2215.0(4)	1828.3(4)	2645(1)	3855(1)	2705.7(4)
Z	2	4	2	2	4	2	2	2	4	4	4	2
D_c/g cm^{-3}	2.031	1.900	2.214	2.137	2.211	2.103	2.373	2.085	1.981	2.191	1.884	1.734
μ(Mo-Kα)/cm^{-1}	19.99	16.98	23.60	21.02	22.89	20.15	26.67	21.19	16.96	23.00	16.39	13.11
Reflections collected	4311	20422	11488	16272	22482	14427	15021	14477	13448	3842	29336	38441
Unique reflections	4047	5021	4476	4942	4931	5043	4622	5148	3540	3608	13272	16724
Observed reflections [$I > 3\sigma(I)$]	2973	3816	3727	4577	2795	3314	4067	2434	3099	2091	8664	2969
R	0.048	0.028	0.042	0.032	0.035	0.034	0.031	0.074	0.030	0.033	0.033	0.039
R'	0.052	0.037	0.050	0.047	0.042	0.043	0.045	0.085	0.048	0.033	0.037	0.045
Goodness of fit, S	2.12	1.67	1.82	1.72	1.56	1.32	1.27	1.80	1.97	1.31	1.15	0.92

33 mg, 0.038 mmol) (Found: C, 28.8; H, 1.60; N, 3.4. Calc. for $C_{21}H_{12}N_2O_{11}Ru_4$: C, 28.91; H, 1.39; N, 3.21%).

Oxidation of complex 3a

A solution of complex **3a** (50 mg, 0.058 mmol) and ferrocenium salt (21 mg, 0.064 mmol) in distilled MeCN (50 ml) was stirred at room temperature for 8 h and the solvent then removed *in vacuo*. The residue was redissolved in CH_2Cl_2 (2 ml) and separated by preparative TLC using the eluent *n*-hexane–dichloromethane (3:1, v/v) to afford a mixture of **9a** and **9a′** (R_f 0.3, 25.4 mg, 0.029 mmol) in 50% yield along with a small amount of **2a** and **3a**.

Reaction of complexes 9a and 9a′ with PPh_3

A solution of complex **9a** (20 mg, 0.023 mmol) in CH_2Cl_2 (30 ml) was stirred with PPh_3 (6.6 mg, 0.025 mmol) at room temperature under an argon atmosphere. Stirring was continued for 1 h, then the solution was concentrated to about 2 ml. Chromatography on silica with *n*-hexane–dichloromethane (3:1, v/v) afforded only one major band accompanied by a very small amount of **9a** and **9a′**. The product was **10a** (R_f 0.75, 23.8 mg, 0.022 mmol, 95%) (Found: C, 40.8; H, 2.4; N, 1.1; P, 2.9. Calc. for $C_{37}H_{24}NO_{11}PRu_4$: C, 40.63; H, 2.21; N, 1.28; P, 2.83%).

Reaction of complex 3a and PPh_3 in the presence of Me_3NO

Compound **3a** (50 mg, 0.058 mmol) and PPh_3 (16.8 mg, 0.064 mmol) were dissolved in CH_2Cl_2 (30 ml) to give a yellow solution. A CH_2Cl_2 solution (20 ml) of Me_3NO (4.8 mg, 0.064 mmol) was added dropwise. After completion of the addition, the mixture was stirred for 15 min. The final solution was then filtered through silica. The filtrate was concentrated to 2 ml. The residue was subject to TLC using *n*-hexane–dichloromethane (3:1, v/v) as eluent. In order of elution, the products were characterized as **10a** (R_f 0.75, 19.1 mg, 0.017 mmol, 30%) and **11a** (R_f 0.55, 15.4 mg, 0.012 mmol, 20%) (Found: C, 48.6; H, 3.1; N, 1.0; P, 2.5. Calc. for $C_{54}H_{39}NO_{10}P_2Ru_4$ **11a**: C, 48.84; H, 2.96; N, 1.05; P, 2.33%).

Reaction of complex 3a with iodine

Compound **3a** (10 mg, 0.012 mmol) was dissolved in CH_2Cl_2 (30 ml). Iodine (1.1 equivalents, 3.3 mg, 0.013 mmol) dissolved in CH_2Cl_2 (20 ml) was gradually introduced to the solution at room temperature over 1 h. The mixture was stirred for 2 h with IR monitoring. After reducing the volume, the residue was separated by preparative TLC on silica, with an eluent of *n*-hexane–dichloromethane (1:1, v/v). Only a small amount of starting **3a** was isolated.

Reaction of complex 3a with iodide

A solution of complex **3a** (10 mg, 0.012 mmol) and $^nBu_4NI$ (4.7 mg, 0.013 mmol) in CH_2Cl_2 (30 ml) was refluxed for 3 h. The initial yellow solution changed to orange upon heating. Then the mixture was dried under reduced pressure and the residue chromatographed on silica using pure CH_2Cl_2 as eluent. The broad orange band with $R_f = 0.25$ was subjected to mass spectrometry after extraction. An ion peak at *m/z* 958 was observed in the negative FAB mass spectrum. It was proposed to be $[Ru_4(CO)_{10}(NOMe)(HC_2Ph)I]^-$ (10.6 mg, 0.011 mmol, 95%).

Reaction of complex 3a with $[N(PPh_3)_2][BH_4]$

A mixture of complex **3a** (10 mg, 0.012 mmol) and 1.1 equivalents of $[N(PPh_3)_2][BH_4]$ (7.1 mg, 0.013 mmol) was refluxed in THF (20 ml) for 3 h. The solvent was then removed under reduced pressure and the residue washed twice with *n*-hexane. Since the orange residue was air-sensitive it could not be further purified by TLC. The compound exhibited a peak envelope at *m/z* 804 with stepwise losses of carbonyls in its negative FAB mass spectrum, which corresponded to $[M - CO]^-$, thus the $[Ru_4(CO)_9(NOMe)(HC_2Ph)H]^-$ ion was suggested.

Attempted hydrogenation on complex 3a

Compound **3a** (20 mg, 0.023 mmol) was dissolved in *n*-hexane (20 ml). The yellow solution was then hydrogenated under reflux. The reaction was monitored by IR spectroscopy and spot TLC. However, no change was observed. About 90% of starting material was recovered upon separation on preparative silica plates.

Reaction of complex 4a with $[N(PPh_3)_2][BH_4]$

Complex **4a** (10 mg, 0.011 mmol) and $[N(PPh_3)_2][BH_4]$ (6.9 mg, 0.012 mmol) were stirred in THF (30 ml) for 3 h. The solvent was then removed *in vacuo* and the residue washed twice with *n*-hexane under argon. The compound left exhibited a peak envelope at *m/z* 860 in its negative FAB mass spectrum, which corresponds to the $[Ru_4(CO)_{10}\{NC(O)OMe\}(HC_2Ph)H]^-$ ion. The orange residue was found to be air-sensitive; further characterization was thus hindered.

Crystallography

Crystals suitable for X-ray analyses were glued on glass fibres with epoxy resin or sealed in a 0.3 mm glass capillary. Intensity data were collected at ambient temperature either on a Rigaku-AFC7R diffractometer (complexes **2a** and **9a**) or a MAR research image plate scanner (complexes **2b**–**5a**, **7b**, **8a**, **10a**, **11a**) equipped with graphite-monochromated Mo-Kα radiation ($\lambda = 0.710\ 73$ Å) using ω–2θ and ω scan types, respectively. Details of the intensity data collection and crystal data are given in Table 6. The diffracted intensities were corrected for Lorentz-polarization effects. The ψ scan method was employed for semiempirical absorption corrections for **2a** and **9a**,[28] however an approximation to absorption correction by inter-image scaling was applied for **2b**–**5a**, **7b**, **8a**, **10a**, **11a**. Scattering factors were taken from ref. 29(*a*) and anomalous dispersion effects[29b] were included in F_c. The structures were solved by direct methods (SIR 88[30] for **2b**–**5a**, **7b**, **8a**, **10a**; SIR 92[31] for **2a**; SHELXS 86[32] for **9a** and DIRDIF[33] for **11a**) and expanded by Fourier-difference techniques. Atomic coordinates and thermal parameters were refined by full-matrix least-squares analysis on *F*, with the ruthenium atoms and non-hydrogen atoms being refined anisotropically. The hydrogen atom of the nitrene moieties and metal hydride were located by Fourier-difference synthesis while those of the organic moieties were generated in their ideal positions (C–H 0.95 Å). Calculations were performed on a Silicon-Graphics computer, using the program package TEXSAN.[34]

CCDC reference number 186/1211.

Acknowledgements

We gratefully acknowledge financial support from the Hong Kong Research Grants Council and the University of Hong Kong. E. N.-M. H. acknowledges the receipt of a postgraduate studentship administered by the University of Hong Kong.

References

1 M. Pizzotti, S. Cenini, C. Crotti and F. Demartin, *J. Organomet. Chem.*, 1989, **375**, 123.
2 S.-H. Han, G. L. Geoffroy and A. L. Rheingold, *Organometallics*, 1986, **5**, 2561; 1987, **6**, 2380.
3 G. D. Williams, G. L. Geoffroy, R. R. Whittle and A. L. Rheingold, *J. Am. Chem. Soc.*, 1985, **107**, 729; G. D. Williams, R. R. Whittle, G. L. Geoffroy and A. L. Rheingold, *J. Am. Chem. Soc.*, 1987, **109**, 3936.
4 M. L. Blohm and W. L. Gladfelter, *Organometallics*, 1986, **5**, 1049.
5 J.-S. Song, S.-H. Han, S. T. Nguyen, G. L. Geoffroy and A. L. Rheingold, *Organometallics*, 1990, **9**, 2386.

6 K. K.-H. Lee and W.-T. Wong, (*a*) *J. Chem. Soc.*, *Dalton Trans.*, 1996, 1707; (*b*) *Inorg. Chem.*, 1996, **35**, 5393.
7 E. N.-M. Ho and W.-T. Wong, *J. Chem. Soc.*, *Dalton Trans.*, 1998, 513.
8 R. D. Adams, J. E. Babin, M. Tasi and T. A. Wolfe, *Oganometallics*, 1987, **6**, 2228.
9 K. Knoll, O. Orama and G. Huttner, *Angew. Chem.*, *Int. Ed. Engl.*, 1984, **23**, 976.
10 P. Mathur, S. Ghosh, M. M. Hossain, C. V. V. Satyanarayana, A. L. Rheingold and G. P. A. Yap, *J. Organomet. Chem.*, 1997, **538**, 57.
11 J. Lunniss, S. A. MacLaughlin, N. J. Taylor, A. J. Carty and E. Sappa, *Organometallics*, 1985, **4**, 2066; J. F. Corrigan, S. Doherty, N. J. Taylor and A. J. Carty, *Organometallics*, 1992, **11**, 3160; 1993, **12**, 1365.
12 A. J. Gordon and R. A. Ford, *The Chemist's Companion: A Handbook of Practical Data, Techniques, and References*, Wiley, New York, 1972, p. 299.
13 R. D. Adams, J. E. Babin and M. Tasi, *Inorg. Chem.*, 1987, **26**, 2807.
14 R. D. Adams, I. T. Horvath and L.-W. Yang, *J. Am. Chem. Soc.*, 1983, **105**, 1533.
15 M. L. Blohm, D. E. Fjare and W. L. Gladfelter, *Inorg. Chem.*, 1983, **22**, 1004.
16 M. L. Blohm and W. L. Gladfelter, *Organometallics*, 1985, **4**, 45.
17 M. Tachikawa, J. Stein, E. L. Muetterties, R. G. Teller, M. A. Beno, E. Gebert and J. M. Williams, *J. Am. Chem. Soc.*, 1980, **102**, 6648.
18 R. Hourihane, T. R. Spalding, G. Ferguson, T. Deeney and P. Zanello, *J. Chem. Soc.*, *Dalton Trans.*, 1993, 43.
19 S. Martinengo, G. Ciani and A. Sironi, *J. Am. Chem. Soc.*, 1982, **104**, 328.
20 R. S. Dickson, R. J. Nesbit, H. Pateras, W. Baimbridge, J. M. Patrick and A. H. White, *Organometallics*, 1985, **4**, 2128.
21 R. E. Stevens and W. L. Gladfelter, *J. Am. Chem. Soc.*, 1982, **104**, 6454.
22 J. A. Smieja, R. E. Stevens, D. E. Fjare and W. L. Gladfelter, *Inorg. Chem.*, 1985, **24**, 3206.
23 R. E. Stevens, R. D. Guettler and W. L. Gladfelter, *Inorg. Chem.*, 1990, **29**, 451.
24 R. E. Stevens and W. L. Gladfelter, *Inorg. Chem.*, 1983, **22**, 2034.
25 K. H. Whitmire and D. F. Shriver, *J. Am. Chem. Soc.*, 1981, **103**, 6754.
26 D. E. Fjare and W. L. Gladfelter, *J. Am. Chem. Soc.*, 1984, **106**, 4799.
27 D. M. Duggan and D. N. Hendrickson, *Inorg. Chem.*, 1975, **14**, 955.
28 A. C. T. North, D. C. Phillips and F. S. Mathews, *Acta Crystallogr.*, *Sect. A*, 1968, **24**, 351.
29 D. T. Cromer and J. T. Waber, *International Tables for X-Ray Crystallography*, Kynoch Press, Birmingham, 1974, vol. 4; (*a*) Table 2.2B; (*b*) Table 2.3.1.
30 M. C. Burla, M. Camalli, G. Cascarano, C. Giacovazzo, G. Polidori, R. Spagna and D. Viterbo, *J. Appl. Crystallogr.*, 1989, **22**, 389.
31 A. Altomare, M. C. Burla, M. Camalli, M. Cascarano, C. Giacovazzo, A. Guagliardi and G. Polidori, *J. Appl. Crystallogr.*, 1992, **25**, 310.
32 G. M. Sheldrick, *Crystallographic Computing 3*, eds. G. M. Sheldrick, C. Kruger and R. Goddard, Oxford University Press, 1985, p. 175.
33 P. T. Beurskens, G. Admiraal, G. Beurskens, W. P. Bosman, S. Garcia-Granda, R. O. Gould, J. M. M. Smits and C. Smykalla, the DIRDIF program system, Technical Report of the Crystallography Laboratory, University of Nijmegen, 1992.
34 TEXSAN, Crystal Structure Analysis Package, Molecular Structure Corporation, Houston, TX, 1985 and 1992.

Paper 8/06091F